Hydrol. Earth Syst. Sci. Discuss., 12, 13069–13122, 2015
www.hydrol-earth-syst-sci-discuss.net/12/13069/2015/
doi:10.5194/hessd-12-13069-2015

Hydrology and Earth System Sciences
Discussions
Open Access

A three-pillar approach to assessing climate impacts on low flows

G. Laaha[1], **J. Parajka**[2], **A. Viglione**[2], **D. Koffler**[1], **K. Haslinger**[3], **W. Schöner**[4], **J. Zehetgruber**[1], and **G. Blöschl**[2]

[1]Institute of Applied Statistics and Computing, University of Natural Resources and Life Sciences (BOKU), Vienna, Austria
[2]Institute for Hydraulic and Water Resources Engineering, Vienna University of Technology, Vienna, Austria
[3]Climate Research Department, Central Institute for Meteorology and Geodynamics, Vienna, Austria
[4]Department of Geography and Regional Science, University of Graz, Graz, Austria

Received: 7 November 2015 – Accepted: 2 December 2015 – Published: 15 December 2015

Correspondence to: G. Laaha (gregor.laaha@boku.ac.at)

Published by Copernicus Publications on behalf of the European Geosciences Union.

Abstract

The objective of this paper is to present a new strategy for assessing climate impacts on low flows and droughts. The strategy is termed a three-pillar approach as it combines different sources of information. The first pillar, trend extrapolation, exploits the temporal patterns of observed low flows and extends them into the future. The second pillar, rainfall–runoff projections uses precipitation and temperature scenarios from climate models as an input to rainfall–runoff models to project future low flows. The third pillar, stochastic projections, exploits the temporal patterns of observed precipitation and air temperature and extends them into the future to drive rainfall–runoff projections. These pieces of information are combined by expert judgement based on a synoptic view of data and model outputs, taking the respective uncertainties of the methods into account. The viability of the approach is demonstrated for four example catchments from Austria that represent typical climate conditions in Central Europe. The projections differ in terms of their signs and magnitudes. The degree to which the methods agree depends on the regional climate and the dominant low flow seasonality. In the Alpine region where winter low flows dominate, trend projections and climate scenarios yield consistent projections of increasing low flows, although of different magnitudes. In the region north of the Alps, consistently small changes are projected by all methods. In the regions in the South and Southeast, more pronounced and mostly decreasing trends are projected but there is disagreement in the magnitudes of the projected changes. These results suggest that conclusions drawn from only one pillar of information would be highly uncertain. The three-pillar approach offers a systematic framework of combining different sources of information aiming at more robust projections than obtained from each pillar alone.

HESSD
12, 13069–13122, 2015

1 Introduction

Streamflow regimes are changing around the world due to human intervention. Low flows are often particularly affected. Direct human impacts such as abstractions or storage effects are not quite easy to quantify. Forecasts of the impacts of a changing climate are even more difficult (Blöschl and Montanari, 2010). Yet, the quantification of future water resources is a key requirement for water management. An increasing number of studies has therefore been conducted in recent years to assess climate change impacts on low flows and streamflow droughts. From a modelling perspective, and also from a systemic one, these studies fall into two groups of approaches (Sivapalan et al., 2003).

The first group of studies assesses climate impacts from observed streamflow records. This is sometimes termed a data-driven or downward approach. As discussed in Sivapalan et al. (2003) the defining feature of the downward approach to hydrologic modelling is the attempt of predicting catchment functioning based on an interpretation of the observed response of the catchment. The approach provides a systematic framework of learning from data, including the testing of hypotheses at every step of analysis. In the context of hydrological change and low flows, the downward approach usually involves statistical trend analyses of observed low flow characteristics such as the annual minima. There has been a considerable number of low flow trend studies across Europe and around the world, including Giuntoli et al. (2013) for France, Hannaford and Buys (2012) for UK, Wilson et al. (2010) in Nordic Countries, Lorenzo-Lacruz et al. (2012) for the Iberian peninsula, and Lins and Slack (1999) and Douglas et al. (2000) for the US. Trend testing is usually performed on a station-by-station basis. Often, the studies are therefore not fully conclusive at the larger scale of climate processes. Only a few studies tested trends in a regional context, using field significance statistics or block-bootstrapping procedures (e.g. Renard et al., 2008; Wilson et al., 2010), while other studies interpret trend patterns rather than significance levels which avoids assumptions of spatial correlations but makes the results less comparable with other studies (e.g. Stahl et al., 2010). An important step in the downward approach is the interpretation of detected trends in order to gain an understanding of the processes giving rise to observed changes. At least some interpretation of low flow trends in the context of climate variables is usually performed, either relative to observed changes or to projected changes. Most studies, however, perform trend interpretations in the sense of a plausibility control rather than in a deductive way, therefore not exploiting the full potential of the downward approach.

The second group of studies simulates future changes from climate scenarios. From a systemic perspective, this may be termed a mechanistic or upward approach, as physically-based models are used to generate climate projections. When the focus is on river flows, model cascades of atmospheric-land surface-catchment models are usually employed. General Circulation Models (GCMs) simulate the climate system's future response to emission scenarios and other human activities that affect the climate system. The GCM outputs are then downscaled to the scale of the catchment of interest, and the resulting projections of climate variables such as precipitation and air temperature are used as inputs of a hydrological model to project streamflow. Applications of the upward approach to streamflow projections are numerous, but relatively few of these studies focus on low flows. These few examples include large river basin studies such as De Wit et al. (2007) for the Meuse, Hurkmans et al. (2010) for the Rhine, and Majone et al. (2012) for the Gállego river in Spain. All of these studies used distributed or gridded hydrological models to simulate the projected response of the entire basin. Similar to the downward approach, regional studies are rare. Large national studies include Wong et al. (2011) for Norway, Prudhomme et al. (2012) for Britain, Chauveau et al. (2013) for France, and Blöschl et al. (2011) for Austria. These studies make use of readily available regionalised rainfall–runoff models developed in prior studies to assess regional patterns of low flow indices. Often, these models are not specifically parameterised for low flows, and therefore associated with higher uncertainty. An alternative approach consists of using global hydrological models instead of regionalised rainfall–runoff models at the end of the model cascade (Prudhomme

HESSD
12, 13069–13122, 2015

et al., 2014). Global models make it easier to understand large-scale changes but the projections are coarser with respect to both spatial scale and the degree of process realism.

Both approaches have their strengths and weaknesses (see Hall et al., 2014) for a comparison of the two methods in the context of floods). The downward approach is the method with a minimum number of assumptions, since it is directly based on observations. If the data are reliable, recent changes of the low flow regime can be related to a changing climate. Recent changes in air temperature have been quite consistent over time in many parts of the world. In the European Alps, for example, the increase in air temperature since 1980 has been about 0.5 °C decade^{-1} with little variation between the decades (Böhm et al., 2001; Auer et al., 2007). If one assumes that air temperature is the main driver of low flows and air temperature changes will persist into the near future in the same way as in the past, one can also assume that observed low flow changes can be extrapolated into the near future. Of course, such an extrapolation hinges on the realism of the assumptions and is likely to be applicable only to a limited time horizon. Also, reliable runoff data over the past five decades are needed. In its own right, such low flow extrapolations may therefore not be very conclusive in terms of future low flow changes.

The alternative, upward approach exploits information from global and regional climate models to project future low flows as a consequence of climate change. An advantage of GCMs is their process basis and their ability to perform multiple simulation experiments for different greenhouse gas emissions scenarios or shared socio-economic pathways. These simulations can be useful for gaining an understanding of the major controls of climate variables and the range of possible projections. However, their spatial resolution is rather coarse (e.g. 10 km for the dynamically downscaled reclip:century simulations used in this study), so small-scale climate features, such as cloud formation and rainfall generation, cannot be resolved. Also one cannot test such projections as they extend into the future. The consequence is that air temperature projections from climate models tend to be robust, while precipitation projections tend to exhibit considerable uncertainties. If precipitation is the main driver of low flow changes, these uncertainties translate into large uncertainties in projected low flows. The uncertainties may be particularly large in complex terrain, such as Alpine landscapes and adjacent transition zones, where climate models are least reliable (Field and Intergovernmental Panel on Climate Change, 2012; Haslinger et al., 2013). Low flow projections may, therefore, vary wildly between scenarios and models for the same region so, again, may not be very conclusive of climate change impacts when taken by itself.

2 Three-pillar approach

The upward and downward approaches have complementary strengths and weaknesses. Importantly they use different sources of information. If a single approach is used, not the entire spectrum of information that may be available is exploited. Current trend studies focus on trend tests, on spatial patterns, or on temporal aspects of trends, but do not combine these aspects with information from climate scenarios. In a similar way, rainfall–runoff projections typically use climate scenarios, but we are not aware of any studies that also exploit the information of the observed low flow time series. Consequently, there may be substantial value in combining the upward and downward approaches in order to build on their respective strengths. The value of combining different pieces of information has been demonstrated by Gutknecht et al. (2006), Merz and Blöschl (2008) and Viglione et al. (2013) in the context of flood estimation.

In this paper we propose combining the most relevant pieces of information contained in low flow observation, climate observations and climate projections using a three-pillar approach (Fig. 1). The first pillar is the assessment of trends in the low flow observations. If observed trends are related to climate, continuing trends may be a realistic scenario for the near future. The second pillar is rainfall–runoff projections based on climate scenarios. If the downscaled GCM signal is reliable, the coupled model will give projections of future catchments response. As these pillars do not fully exploit the information of locally observed climate, we add a third pillar of stochastic

HESSD
12, 13069–13122, 2015

rainfall–runoff projections based on local climate observations. This pillar is anticipated to facilitate interpretation of past trends and trend-based extrapolations into the future and assist in linking the other two pillars with each other.

The three-pillar approach allows us to assess climate impacts from independent sources of information each of which may have different error structures. The combination of the individual assessments therefore opens up a number of opportunities. The first opportunity is to obtain a judgement about the credibility of the individual approaches. This is achieved by comparing observed and simulated low flow time series. Low flow observations will generally be most reliable as they provide direct measurements of the variable of interest. Hence, they can be used to assess the performance of stochastic projections and climate models for the observation period, i.e. without assumptions about the future development. This provides insight into the predictive performance of the rainfall–runoff model during the calibration period and its skill of tracing changes of the climate signal down to low flows (dynamic performance). On the other hand, the comparison may yield insight into the GCM performance, as reanalysis runs contain all necessary information to get an appreciation of the realism of (downscaled) GCM signals, when being compared to observed climate and runoff signals. However, also low flow observations may be inaccurate and trends may be artefacts from instrumentation changes or the limited observation window. The mutual comparison of observed low flows with the rainfall–runoff reanalysis offers the opportunity of verifying trends in both climate and runoff signals, as a solid basis for future projections.

The second opportunity offered by the three-pillar approach is to better understand the response of low flow regimes to climate change. This is achieved by comparing climate signals and runoff signals. Such an analysis may first focus on the observation period in order to understand observed changes of the low flow regime. In a second step, the analysis may be extended to the future, in order to put projected changes into the context of the past. Low flows are a result of the complex interactions of climate drivers with catchment processes, so a direct comparison of climate and low flows may be difficult. A stochastic rainfall–runoff projection method may assist in such a com-

HESSD
12, 13069–13122, 2015

parison as it can trace low flow trends back to trends in the meteorological variables. A stochastic rainfall and temperature model typically decomposes meteorological signals into components such as linear trends and cyclical fluctuations. The joint analysis of these components with the low flow signal may yield insight into the co-behaviour of low flows and climate variables in cases where low flow signals are contaminated by noise. From the analysis we can expect a better understanding of climate change dynamics, and of the resilience and sensitivity of low flow generation processes to changes in the climate conditions.

Thirdly, the three-pillar approach offers a more complete way of assessing the uncertainty of projections than each of the pillars alone. This is because one can safely assume that the errors are, at least partly, disjoint because of the different data sources. Given the substantial uncertainty associated with climate impact studies, more detailed information on the uncertainty is certainly attractive, even though a full assessment is likely not possible given the partial information available in such studies. For rainfall–runoff projections the sources of uncertainty include their sensitivity to climate scenarios, climate model and downscaling errors, and the prediction uncertainty of the rainfall–runoff models themselves which arise from the model structure and parameters. The latter are related to the choice of the objective function and the calibration period. For trend studies, uncertainty can be assessed by statistical significance tests, subject to the assumptions made, and by confidence bounds of trends.

All of the opportunities combine the information of the three pillars in some way. Of course, the idea of combining different sources information has already often been used and tested in hydrology. Examples include the combination of local and regional hydrological information (e.g. Kuczera, 1982; Stedinger and Tasker, 1985), short and long low flow records (e.g. Laaha and Blöschl, 2007), hard and soft hydrological information (e.g. Winsemius et al., 2009), and uncertainty estimates in ungauged basins based on the downward and upward approaches (Gupta et al., 2013). The combination can be based on formal methods (e.g. Viglione et al., 2013) which typically assume that the different pieces of information are all random samples from the same distribu-

HESSD
12, 13069–13122, 2015

tion, and they differ only due to their sampling variability. The distribution of the entire population is then estimated by Bayesian or other methods. As an alternative, expert judgement can be used to combine the different sources of information (e.g. Merz and Blöschl, 2008). The disadvantage is that it is less objective but the advantage is its flexibility as it is based on a reasoning on the strengths and weaknesses of the individual pillars. In this paper, we use expert judgement to combine the findings from the three pillars.

In Sects. 4–6 we present the methods and assessments for each pillar separately. The strategy and application of the synthesis method are presented in Sect. 7, followed by discussion and conclusions. The three-pillar approach offers a systematic way of obtaining an overall assessment of future climate impacts, including an appreciation of the reliability of each method gleaned from the consistence of the pillars. We illustrate the viability of the approach for four example regions in Austria and discuss the findings in the context of hydrological climate impact studies.

3 Example data set

3.1 Study regions and hydrologic data

The four example regions used here to illustrate the three-pillar approach are representative of the main climatological units in Austria. In each of them a typical catchment was selected which are a subset of a classification ("low flow hot-spots") used in previous low flow and drought studies (Haslinger et al., 2014; Van Loon and Laaha, 2015). Although Austria is highly diverse with respect to climate and physiography, each of the regions is rather homogeneous in terms of climate and the hydrological regime.

The first region is located in the Alps and exhibits a clear winter low flow regime. Freezing is the driving factor of low flows in this region, so long-term trends may be expected to be related to changing air temperatures. The region, termed Hoalp in the following (for Hochalpen), is represented by the catchment of the Matreier Tauernhaus

Discussion Paper | Discussion Paper | Discussion Paper | Discussion Paper |

HESSD

12, 13069–13122, 2015

stream gauge at the Tauernbach (area is 60 km^2, altitude is 1502 m a.s.l., observation period is 1951–2010).

The second region is located north of the Alps with a dominant summer low flow regime. The region exhibits a quite humid climate as it receives substantial precipitation from northern and western air masses. Seasonal precipitation deficits are the driving forces of low flows so long-term trends are likely related to changes in precipitation and temperature. The region, termed Muhlv in the following (for Mühlviertel), is represented by the catchment of the Hartmannsdorf stream gauge at the Steinerne Mühl (area is 138 km^2, altitude is 500 m a.s.l., observation period is 1956–2010).

The third region is located south of the Alps, and also exhibits a dominant summer low flow regime. Precipitation enters the area from the Northwest through Atlantic cyclones, although screened to some extent by the Alps, as well as from the South through Mediterranean cyclones, which is particularly the case in autumn. Again, seasonal precipitation deficits are the driving forces of low flows so long-term trends tend to be related to changes in precipitation and temperature. The region, termed Gurk in the following (for Gurktal), is represented by the catchment of the Zollfeld streamgauge at the Glan (area is 432 km^2, altitude is 453 m a.s.l., observation period is 1965–2010).

The fourth is located in the Southeast of Austria. This region is situated in the lee of the Alps, at the transition to a Pannonic climate. The precipitation is lowest in this region, and low flows exhibit a dominant summer low flow regime. Seasonal precipitation deficits are the driving forces of low flows and so the long-term trends should be related to changes in precipitation and temperature. The region, termed Buwe in the following (for Bucklige Welt), is represented by the catchment of the Altschlaining stream gauge at the Tauchenbach (area is 89 km^2, altitude is 316 m a.s.l., observation period is 1966–2010).

Climate records were used for two out of the three pillars, i.e. the rainfall–runoff-projections and the stochastic simulations. They serve for two purposes.

Firstly, climate records are required for calibrating the hydrological model. Gridded data sets of daily precipitation, air temperature, potential evaporation and snow depth were used. These data sets are based on measurements of daily precipitation and snow depths at 1091 stations and daily air temperature at 212 climatic stations. Potential evapotranspiration was estimated by a modified Blaney–Criddle method based on daily air temperature and potential sunshine duration. For details about the estimation and interpolation methods see Parajka et al. (2007).

Secondly, climate records provide the main input to the stochastic simulations, which are used to decompose the signal of climate drivers in the past as the basis for extrapolations into the future. For this purpose, one climate station was selected for each example catchment in their proximity and at similar altitudes. Precipitation and temperature records over the period 1948–2010 were used for the selected stations.

3.2 Climate simulations

For the rainfall–runoff projections we used four regional climate model (RCM) runs which were selected from the reclip:century 1 project (Loibl et al., 2011). The variability of climate projections is represented by COSMO-CLM RCM runs forced by ECHAM5 and HADCM3 global circulation models and three different IPCC emission scenarios (A1B, B1 and A2). A simple but effective way to check the realism of the ensemble of climate simulations with respect to low flows is to use an index that combines temperature and precipitation signals in a way that represents the climate forcing in low flow generation. One index commonly used in atmospheric drought studies is the Standardized Precipitation Evaporation Index, SPEI (Vicente-Serrano et al., 2010), which represents the total effect of precipitation and temperature changes on the climatic water balance. The SPEI is defined as the Gaussian-transformed standardized monthly difference of precipitation and evapotranspiration based on an accumulation period of one to several months. Values below/above zero indicate deficits/surpluses in the climatic water balance, and values below −1.0 indicate drought conditions. Haslinger et al. (2014) demonstrated that the SPEI is well correlated with summer low flows, and indeed more relevant for low flow generation than precipitation alone.

HESSD
12, 13069–13122, 2015

Figure 2 shows the evolution of SPEI of the four regions stratified by summer and winter months. Each value corresponds to the seasonal (three-month) average of SPEI(1), i.e. the Standardized Precipitation Evaporation Index based on an aggregation period of one month. For the winter months (Fig. 2, lower panels), SPEI remains stable which is equivalent to a stationary precipitation signal. This is because the projected temperature increase is not reflected by the SPEI due to the low evaporation rates in winter. However, the timing of snowmelt is likely to change. For Hoalp and Muhlv, the climate simulations for the winter month fit well to the observations (light red and red lines). For Gurk and Buwe, the climate simulations seem to be somewhat less realistic.

For the summer season, the SPEI simulations suggest much dryer atmospheric conditions in the future, which will decrease the low flows. Overall, the climate simulations do not fit so well to the observations as for the winter, and the plausibility of the projections varies between regions. For the Muhlv region, the SPEI signal fits relatively well to the observations, for Gurk the simulated signal drops somewhat more steeply than expected, and for Buwe the signal is much steeper than the observed signal, which does not show a falling trend over the last 50 years. Interestingly, all summer SPEI graphs are relatively stable until 2050, and drop in the second half of the 21th century. This is mainly due to the characteristics of the ECHAM5 simulations which show only minor precipitation changes until the middle of the century, and after 2050 an enhanced decrease in rainfall. Such an effect is not observed in the other models or ECHAM5 runs, and contributes to the overall uncertainty of the scenario approach. The extremely negative trends in the summer SPEI should also be treated with caution because the potential evapotranspiration calculations within the SPEI algorithm is known to overestimate climate change signals expressed by surface temperature trends (Sheffield et al., 2012). Overall, the SPEI values of climate simulations do suggest decreasing low flows in summer and perhaps stable low flows in winter, although SPEI is less well suited for predicting winter conditions. From the fit to observations, climate simulations seem more realistic for Hoalp and Muhlv, somewhat less realistic for Gurk, and least realistic for Buwe.

HESSD
12, 13069–13122, 2015

4 Observed trends – extrapolation

4.1 Methods

As a starting point, we are interested in evidence for climate change from the low flow observations. Similar to other studies, we performed trend analyses of annual low flow series, using the Sen's slope estimator (e.g. Stahl et al., 2010). Instead of fitting a regression line to all data points simultaneously, the trend is estimated as the median of all slopes between pairs of sample points. This makes the trend estimates insensitive to outliers and more suitable for heteroscedastic data.

For each station, analyses were performed for annual series of the Q_{95} low flow quantile (i.e. the flow that is exceeded 95 % of the time of the respective year). A common observation period (1976–2008) was used to make the trend estimates comparable across gauges. Based on autocorrelation analysis, we decided not to prewhiten the data (remove first order autocorrelation effects from the time series) as proposed in some studies, because the serial correlations in the annual low flow series were mostly insignificant. Significance testing of trends was performed using a standard Mann–Kendall test. The results were finally compared with significance statistics of prewhitened series obtained by the Yue Pilon method for trend-free prewhitening (Yue et al., 2002) but there was almost no difference.

Under the assumption that observed changes are linear and persistent, the trends may be extrapolated as a simple, observation-based scenario for future low flows. It is realised that this is quite a strong assumption, which will be more realistic for the near future than for a longer time horizon. Both the estimation of trends and their extrapolation into the future are clearly subject to considerable uncertainty that needs to be considered in the final combination of the three pillars. We therefore estimate expected low flows together with their confidence bounds. We use a simple linear regression estimator of the expected value in a specific year t_0:

$$\hat{Q}_{95}(t_0) = \hat{a} + \hat{b}t_0. \tag{1}$$

HESSD
12, 13069–13122, 2015

Note that in our robust regression framework, $\hat{a}$ and $\hat{b}$ are the Sen-slope estimates of the regression parameters. The uncertainty of the trend estimate is given by the confidence bound of the regression line:

$$Q_{95} \in \left(\hat{a} + \hat{b}t_0 \pm z_{n-2;1-\alpha/2}\, s \sqrt{\frac{1}{n} + \frac{\left(t_0 - \bar{t}\right)^2}{(n-1)\, s_t^2}} \right). \tag{2}$$

Again, $\hat{a}$, $\hat{b}$ are the Sen-slope estimates of the regression parameters, $z_{n-2;1-\alpha/2}$ is the quantile of the Student distribution ($z_{n=33} = 2.04$ for a two-sided 95 % confidence interval), n is the sample size (number of observed years), $\bar{t}$ and s_t^2 the mean and the variance of t.

Making use of the robustness of the Sen-slope estimator, a robust estimate of the error variance s^2 may be obtained from $\hat{b}$ by:

$$s^2 = \frac{(n-1)}{(n-2)} \left(s_Q^2 - \hat{b}^2 s_t^2 \right) \tag{3}$$

where s_Q^2 is the variance of the annual Q_{95} values. As can be seen from the squared term $\left(t_0 - \bar{t}\right)^2$ in Eq. (2), the uncertainty is lowest at the mid-point of the observation period and increases as one moves away from it. The confidence bounds therefore reflect the increasing uncertainty of extrapolations of the observed trends into the future.

4.2 Results

Table 1 summarizes the results of the trend analyses. For two catchments, the trends are significant but with different signs. The Hoalp catchment exhibits a strongly positive trend indicating that the catchment has become wetter over the observation period.

HESSD
12, 13069–13122, 2015

A negative trend is observed for the Buwe catchment, which became dryer. Negative (drying) trends are also observed for the Muhlv and Gurk catchments but these are not significant at the 0.05 level.

While our focus is on the four example catchments, it is important to put the local analyses in a regional context to avoid the detection of local effects on the flow regime, such as anthropogenic impacts. Figure 3 shows trends of the four example gauges used in this study, together with trends at 408 stream gauges in Austria and neighbouring regions. The map indicates characteristic patterns for the study area, which correspond well to the main hydro-climatic units represented by the four catchments. Significant positive trends (increasing discharges) such as in the Hoalp catchment are generally found for the Alpine region. Some negative trends (decreasing discharges) are found in the southeast of Austria and in Upper Austria in the north of the Alps but, here, the number of stations with significant trends is low compared to the total number of stations. Additional regional analyses (not shown here), including field significance testing, confirm the finding that trends in the Southeast are more significant than in the North. The Buwe region appears to be notably affected by climate change as low flows show a strong decrease at the end of the observation period. Trends in the Muhlv region north of the Alps are less severe, as they relate to single catchments and do not show a consistent regional behaviour. Alpine catchments in the Hoalp region, however, seem to have benefited from atmospheric wetting and this trend seems to persist into the future.

Table 2 gives the projections obtained from trend extrapolation for the four catchments together with their confidence bounds. The projections for the period 2021–2050 indicate an increase of low flows in the Hoalp catchment of 42 % if the present trend persists until 2050. The uncertainty of this projection is, however, quite large as indicated by the range of the confidence interval (−5 to 88 %). For the remaining catchments, a decreasing trend is projected which is lowest in Muhlv (−10 %), moderate in Gurk (−36 %), and very strong in Buwe (−89 %). Again, there is substantial uncertainty when extrapolating the trends to the 2050 time horizon. For instance, the confidence

HESSD
12, 13069–13122, 2015

interval of Muhlv ranges from −51 to +32 %, which is a range eight times the expected value of the projected changes. Hence, from the available dataset, trend extrapolation can only provide a very approximate estimate of future low flows. The uncertainty increases when predicting changes for a more distant time horizon of 2080 (Table 2). The extrapolations result in negative values for the discharge of the Buwe basin, indicating that the stream may fall dry during the low flow period. Obviously, one would have very low confidence in the absolute figures of such trend scenarios for the more distant future.

5 Rainfall–runoff projections based on climate scenarios

5.1 Methods

A common method for projecting river discharge regime into the future is the delta change approach (e.g. Hay et al., 2000; Diaz-Nieto and Wilby, 2005). The idea of this concept is to remove biases of regional climate model (RCM) simulations when using them as inputs to hydrologic models. First, a hydrologic model is calibrated for the reference period by using observed climate variables, typically precipitation and air temperature. In the next step, the differences between RCM simulations of the reference (control) and future periods are estimated on a monthly basis. These differences (delta changes) are then added to the observed model inputs and used in the hydrological modelling for simulating the future. The differences between the discharge simulations in the reference and future periods are used to assess potential impacts of a changing climate on future river flows.

A conceptual rainfall runoff model (TUWmodel, Viglione and Parajka, 2014) is used here. The model simulates the water balance components with a daily time step based on precipitation, air temperature and potential evaporation data as inputs. Details on the model structure and applications are given in Parajka et al. (2007) and (Ceola et al. (2015). TUWmodel is calibrated by the SCE-UA automatic calibration procedure

HESSD
12, 13069–13122, 2015

(Duan et al., 1992). The objective function (Z_Q) of the calibration is selected on the basis of prior analyses performed in different calibration studies in the study region (see e.g. Parajka and Blöschl, 2008). It consists of two variants of Nash–Sutcliffe Model efficiency, M_E (Eq. 5) and $M_\mathrm{E}^{\log}$ (Eq. 6) that emphasize high and low flows, respectively. Z_Q is defined as

$$Z_Q = w_Q \cdot M_\mathrm{E} + (1 - w_Q) \cdot M_\mathrm{E}^{\log} \tag{4}$$

where w_Q represents the weight on high flows and $(1 - w_Q)$ the weight on low flows. M_E and $M_\mathrm{E}^{\log}$ are estimated as

$$M_\mathrm{E} = 1 - \frac{\sum_{i=1}^{n} \left(Q_{\mathrm{obs},i} - Q_{\mathrm{sim},i}\right)^2}{\sum_{i=1}^{n} \left(Q_{\mathrm{obs},i} - \overline{Q_\mathrm{obs}}\right)^2} \tag{5}$$

$$M_\mathrm{E}^{\log} = 1 - \frac{\sum_{i=1}^{n} \left(\log\left(Q_{\mathrm{obs},i}\right) - \log(Q_{\mathrm{sim},i})\right)^2}{\sum_{i=1}^{n} \left(\log(Q_{\mathrm{obs},i}) - \overline{\log(Q_\mathrm{obs})}\right)^2} \tag{6}$$

where $Q_{\mathrm{sim},i}$ is the simulated discharge on day i, $Q_{\mathrm{obs},i}$ is the observed discharge, $\overline{Q_\mathrm{obs}}$ is the average of the observed discharge over the calibration (or verification) period of n days.

In order to assess the uncertainty of low flow projections from a modelling perspective, different variants of model calibration were evaluated by varying the weights of Eq. (4), following the methodology of Parajka et al. (2015). In order to assess the impact of time stability of model parameters, TUWmodel was calibrated separately for three different decades (1976–1986, 1987–1997, 1998–2008), following the methodology of Merz et al. (2011).

5.2 Results

Table 3 summarizes the runoff model efficiencies ZQ. The results indicate that the differences in runoff model performance between the calibration decades are rather small. Overall, the largest efficiency is obtained for the Hoalp basin, which is characterised by a very consistent hydrological regime throughout the years (Fig. 4). Snow accumulation and melt have a dominant effect on the hydrologic regime, as they affect the timing of low flow periods in winter and flood events in summer. In contrast, the lowest model efficiency is found for Buwe. The shape of most hydrographs is very flashy and thus very difficult to model on a daily time step. Additionally, there are only two climate stations in the catchments, which makes it difficult to capture local precipitation events such as summer storms. The fast runoff response is caused by shallow soils and efficient drainage (see Gaál et al., 2012). Both low flow periods and floods mainly occur in summer. The event variability is large between and within the years (Fig. 4). As compared to other catchments in Austria (Parajka et al., 2015), the Hoalp and Buwe catchments represent typical conditions with high and low model performance, respectively.

Figure 5 shows the results of the model simulations in terms of annual low flow quantiles Q_{95} in the reference period 1976–2008. The hydrologic model is calibrated for a selected decade, but the model simulations are performed for the entire reference period. The left panels of Fig. 5 show the variability of Q_{95} estimated from 11 variants of objective functions. The range of Q_{95} for the 11 calibration variants is plotted in yellow and blue for the calibration periods 1976–1986 and 1998–2008, respectively, and their overlap is plotted in green.

The right panels show the variability of Q_{95} due to model parameters obtained from different decades for two weightings: $w_Q = 0.5$ (light orange) and $w_Q = 0.0$ (red). Although the model has not been calibrated directly to Q_{95} quantiles, it simulates Q_{95} well in the example basins and the differences between the two weighting variants are small or moderate in absolute terms. The effect of temporal instability of model parameters is clearly visible in the Buwe and Gurk basins, where the model calibrated to the 1976–1986 period tends to overestimate Q_{95} in the period 1998–2008. The decade 1976–1986 represents a colder period with less evapotranspiration and relatively higher runoff generation rates which is reflected by lower values of the soil moisture storage parameter (FC) and lower values of the parameter controlling runoff generation (BETA). The model therefore overestimates runoff when applied to the drier and warmer period 1998–2008.

Figure 5 further shows that the uncertainty of Q_{95} estimates is the largest in the Alpine basin with dominant winter low flow regime. Alpine river regimes are characterised by a greater variability of discharges than low-land regimes (Fig. 4). Because of this, model calibration is more sensitive to the weights assigned to high and low flows. The Alpine basin is also more sensitive to the choice of the calibration period. The strong seasonality of the Alpine regime is a reflection of a high sensitivity of discharge generation to seasonal climate. Decadal climate variation will therefore have a similarly strong effect on discharges and, through discharges, on model calibration. The strong sensitivity to weighting and the calibration period are a result of the highly seasonal regime and make projections in Alpine catchments more uncertain than in lowland catchments. In contrast, the uncertainty is smallest in the Gurk and Buwe basins where, interestingly, the effect of time variability of the model parameters is of similar magnitude as the effect of the weighting in the objective function.

Scenarios of air temperature and precipitation from the four RCM runs are presented in Fig. 6. The largest warming in the four basins is obtained by simulations driven by HADCM3. An increase of more than 2 °C is projected for January and the summer months. The largest difference between the ECHAM5 scenarios occurs in January. While the ECHAM5-A2 run simulates a decrease in mean monthly air temperature, the A1B2 emission scenario projects and increase in monthly air temperature of almost 2 °C in all selected basins. The ECHAM5 scenarios are consistent for the summer months with an increase in air temperature of about 1 °C. The precipitation projections are regionally less consistent and vary mostly around ±15 %. Exceptions are the HADCM3 run which simulates a decrease of almost 30 % in the Gurk and Buwe basins

HESSD
12, 13069–13122, 2015

in August, and the ECHAM5-A1B2 run which simulates an increase of about 30 % in the Hoalp and Muhlv basins in December.

The delta change projections of low flow quantiles Q_{95} are finally presented in Fig. 7. The projections for the period 2021–2050 indicate an increase of low flows (Q_{95}) in the Alpine Hoalp basin, on average in the range of 15 to 30 % and 20 to 45 % for the different climate projections and calibration weightings, respectively. In the Muhlv basin, no significant change in Q_{95} is expected. The median of changes is in the range of ±5 %. Larger decreases are projected for Gurk (7–13 %) and Buwe (15–20 %). A comparison of uncertainty and range of future projections indicates that the estimation of Q_{95} is sensitive not only to the selection of the climate scenarios, but also to the selection of the objective function and the calibration period. The uncertainty is largest in the Hoalp basin, where the selection of the objective function is more important than the selection of climate scenarios. The winter mean air temperature in the Hoalp basin is about −6.0 °C and the projected increases range from 2 to 2.5 °C depending on the scenario. These differences are of little relevance for snow storage and snowmelt runoff during the winter low flow period. A large uncertainty and sensitivity to the choice of objective function and calibration period is also obtained for the Muhlv and Buwe basins. Only in the Gurk basin the sensitivity to the choice of objective function is smaller than the time stability of model parameters. This is a result of the relatively high sensitivity to the calibration period (Fig. 5) in combination with relatively small differences between climate water balances resulting from different scenarios (as reflected by the small spread of SPEI projections in Fig. 2). The projections based on the period 1976–1986 tend to simulate a larger variability of Q_{95} than those calibrated to the period 1998–2008, however the variability is similar to Buwe and Muhl basins.

HESSD
12, 13069–13122, 2015

6 Stochastic projections based on rainfall model extrapolation

6.1 Methods

While in Sect. 4 observed trends of Q_{95} were extrapolated, and in Sect. 5 RCM scenarios were used to anticipate future low-flows, this section adopts a different approach which, conceptually, is between the two. We use a stochastic model to investigate what would happen if the trend of observed precipitation and temperature in the period 1948–2010 would persist into the future. The stochastic model allows us to simulate future time series of climate drivers based on extrapolating components of precipitation and temperature models. These simulations are then employed to drive the rainfall–runoff model of Sect. 5.

The precipitation model used here is the point stochastic model of Sivapalan et al. (2005). The model consists of discrete rainfall events whose arrival times (or interstorm periods), duration and average rainfall intensity are all random, governed by specified distributions whose parameters are seasonally dependent. In this paper, the model was run on a daily time scale. No fractal temporal-downscaling of within-storm rainfall intensities was performed, since the interest was in low flows which are not expected to depend much on within-storm time patterns.

For air temperature, instead, the 100 possible time series were obtained by randomising the observations in the following way. The time series of daily temperatures were detrended according to the observed trend of mean annual temperatures, the years were randomly mixed (with repetition), and the trend was added to the reshuffled series. The trend in the temperatures was reflected by an analogous trend in potential evapotranspiration.

A storm-separation algorithm was applied to the precipitation data of the four stations, based on a minimum duration of dry periods, in order to isolate precipitation events. The temporal trends of three rainfall model parameters (mean annual storm duration, mean annual inter-storm period and mean annual storm intensity) were then

HESSD
12, 13069–13122, 2015

estimated from the event time series with the Theil-Sen algorithm, to serve as trend components in the stochastic precipitation model.

Figure 8 shows that the estimated trend components fit well to the precipitation statistics. Annual mean storm duration decreases quite strongly for the Alpine Hoalp catchment (by about −0.8 days/100 years). There is also a slight decrease for the Gurk (−0.4 days/100 years) and Buwe catchments (−0.3 days/100 years). Interstorm period and storm intensity (Fig. 8, centre and right panels) show no significant changes for most regions, apart from the Gurk catchment where the annual mean interstorm period increases by about 1 day/100 years, and annual mean storm intensity increases by 2 days/100 years. The trends in these precipitation model components were subsequently extrapolated into the future. The remaining rainfall model parameters were calibrated to the precipitation data as described in Viglione et al. (2012) and were kept constant for the entire simulation period. The stochastic rainfall model was finally used to simulate an ensemble of 100 possible time series of precipitation affected by trends in the three model parameters for the period 1948–2080.

6.2 Results

Figure 9 shows the stochastic simulations of mean annual daily precipitation and mean annual temperature for the four example catchments, together with the observed signals. No trends of precipitation (left panels) are visible for Muhlv in the North and Gurk in the South. A drying trend is visible for Buwe in the Southeast and for the Alpine Hoalp catchment, but in the latter case the observations exhibit a rather complex signal which seems not well represented by the model. Temperature simulations (Fig. 9, right panels) correspond much better to the observations. They consistently show increasing trends for the whole study area. The trend is most pronounced in the Alps (+4.4 °C/100 years), somewhat less pronounced in the South and Southeast (+2.8 and +2.6 °C/100 years), and there is only a weak trend in the North (+1.7 °C/100 years).

Figure 10 shows the stochastic projections of annual runoff and Q_{95} (red lines) together with the observations (black line) for part of the period. For the Hoalp region

HESSD
12, 13069–13122, 2015

(Fig. 10, top row) Q_{95} decreases only slightly despite the simulated large decrease of annual runoff and precipitation. This is because winter low flows are more controlled by air temperature which would be expected to increase the low flows, and the two effects essentially cancel. For the Muhlv region (second row in Fig. 10), the model extrapolates a slight reduction of Q_{95} in the future, even though there is hardly any change in the annual precipitation (second row in Fig. 9), which is due to increases in the evapotranspiration. For the Gurk region (third row in Fig. 10), the model also extrapolates a slight decrease in Q_{95}. This change echoes both the increasing trends in evapotranspiration and in the interstorm period (Fig. 9). For the Buwe region (bottom row in Fig. 10) the extrapolated reduction of Q_{95} is quite important. In this case, the annual precipitation slight decreases (Fig. 9), which adds to the effect of the increasing evapotranspiration.

The underlying assumption of observed trends in precipitation and temperature to persist into the future is quite strong. In contrast to Sect. 4, here we do not consider the uncertainty associated with the estimation (and extrapolation) of the trends. The confidence bounds in Figs. 10 and 11 are associated with the modelled variability of the low-flow producing processes, as represented by the stochastic precipitation and temperature models, which are assumed to be known both in the present and in the future. Despite the strong assumption made, it should be noted that the results of this approach are non-trivial and very interesting in their own right. For instance, the way trends in precipitation and temperature translate into trends in low-flows differs between the catchments because of the nonlinear hydrological processes interactions between precipitation and temperature.

7 Three-pillar synthesis

7.1 Combination of information

The individual analyses project low flow changes from different sources of information. The first pillar, trend extrapolation, exploits the temporal patterns of observed low

HESSD
12, 13069–13122, 2015

flows and extrapolates them into the future. The second pillar, rainfall–runoff projections is based on climate scenarios of precipitation and temperature to drive a rainfall–runoff model. The third pillar, stochastic projections, exploits the temporal patterns of observed precipitation and temperature and extrapolates them into the future in a stochastic way to drive a rainfall–runoff model. From the assessments it is clear that the individual projections are rather uncertain because of limited data and uncertain models or assumptions.

The methods and information used in each pillar are largely independent from each other, so one would also expect the errors to be close to independent. A combination of the projections should therefore increase the overall reliability of the projection. The combination is achieved here by hydrological reasoning based on a visual comparison of synoptic plots of individual estimates and their respective confidence bounds. The reasoning accounts for the differences in the nature of the uncertainties of the projections and gives more weight to the more reliable pieces of information.

When combining the projections two cases exist. In the first case, projections are consistent within their confidence bounds. This will lend credence to all projections as they support each other. The confidence one has in the projection will depend on how strongly the pillars agree, and on their individual uncertainties. The overall uncertainty will be expressed here as three levels of confidence (high, medium, low), which is in accordance with the uncertainty concept of the IPCC report (Field and Intergovernmental Panel on Climate Change, 2012).

In the second case, the individual projections are not consistent within their uncertainty bounds which will suggest lower confidence in the overall projections. Rather than simply averaging the individual projections, here, the analysis aims at understanding the reasons for the disagreement, by checking the credibility of each projections based on the data used and the assumptions made. The confidence bounds of the individual projections are a starting point for assessing the credibility of each pillar. Additionally, the plausibility of the precipitation and temperature scenarios simulated by the climate model can be checked by comparing them with the observations. The plausibility of the trend extrapolations can be checked, at least for the immediate future, by examining the consistency of the trend within the observations.

7.2 Application to the study area

The synthesis plots for the four regions in Austria are presented in Fig. 11. Each panel provides a synoptic view of the three pillar projections. Observed annual low flows as plotted as black lines. Trend estimates and confidence bounds are plotted as blue lines. As can be seen, the uncertainties increase drastically with the extrapolation length.

The climate scenario based rainfall–runoff projections are given as box plots representing the averages of each of the two time horizons, 2021–2050 and 2051–2080. The ranges of the box plots indicate different parameters of the hydrological model, and colours indicate climate scenarios. Model simulations for the observation period are shown as grey lines. They allow conclusions about the performance of the rainfall–runoff modelling.

Finally, the red lines represent the stochastic simulation runs for the past and the future from which confidence bounds (dashed and dotted lines) were calculated.

For the Hoalp region in the Alps (Fig. 11, top left), both the extrapolation of observed low flow trends and the climate scenario based rainfall–runoff projections suggest increases in low flows. In this region, low flows occur in winter due to snow storage processes which are mainly driven by seasonal temperature. This process should be captured well by the climate scenarios, which tend to simulate temperatures more accurately than precipitation. In fact, Schöner et al. (2012) showed that the temperature scenarios correspond well with the observed increase of winter temperature in the Alpine region since the 1970s. The plot does show that the rainfall–runoff projections from different parameterisations vary strongly. This uncertainty is mainly due to the lower low flow performance of rainfall–runoff models in Alpine landscapes. From a regional perspective, the observed low flow trends are significant, i.e. the percentage of stations with a trend is significantly greater than expected by chance (Blöschl et al., 2011; Laaha at al., 2015). This finding adds credence to the low flow trend extrapolation, as on can assume that the observed air temperature trends will persist into the future. The stochastic projections, in contrast, predict a slightly decreasing low flow trend which is inconsistent with the other two pillars. A closer inspection of the stochastic model components suggests that the temperature trends in the Alps are not captured well by the model. This is because the model is based on annual temperature parameters, but the winter temperature changes do differ from those of the annual means. Of course, the model could be straightforwardly extended to include seasonal variations in the changes but, as it is now, it nicely illustrates the case of an inconsistency that is well understood. Because of this, little weight is given to the stochastic projections in the overall assessment. From the combined information of observed low flow trends and climate projections of low flows one would expect an increase in low flows by at least 20–40 % for the 2020–2050 period (medium to high confidence) and an increase by at least 30–50 % for the 2050–2080 period (medium confidence).

For the Muhlv region north of the Alps, the extrapolation of observed low flow trends corresponds well with the stochastic projections (Fig. 11, top right). Both methods project a slightly decreasing trend, corresponding to a reduction of about 5–10 % for the 2020–2050 period. The rainfall–runoff simulations capture the observed trend well for the observation period so also the future simulations will likely be reliable in terms of the hydrological processes. From the climate scenarios a slight increase in Q_{95} for the near future would be projected. This is somewhat contradictory to the trend extrapolation and stochastic projections but still lies in the confidence bounds of these methods. Low flows in this region occur in summer and are therefore more precipitation-driven than temperature-driven, so the climate scenario based rainfall–runoff projections are likely less reliable. On a regional level, Blöschl et al. (2011) and Laaha et al. (2015) reported little significance of the observed low flow trends which fits well into the findings of the three-pillar projections. Overall there is perhaps a slight tendency for decreasing discharges in the 2020–2050 period but this trend is not strong. This conclusion is relatively certain (medium confidence) because of the good agreement of all individual assessments. For the 2050–2080 period further in the future, the low flow trend extrapolation will be less reliable, as reflected by the wide confidence bounds, but it is consistent with the decreasing trend of the stochastic projections. The climate scenario based rainfall–runoff projections suggest a stronger drying trend, corresponding to a reduction of about 50–60 %. The range of different rainfall–runoff projections is outside the confidence bounds of the stochastic projections. Low flows are precipitation-driven in this area and so the confidence in the rainfall–runoff projections should be low. Overall, this suggests a slight drying trend for the 2050–2080 period (low to medium confidence).

The Gurk region south of the Alps (Fig. 11, bottom left) shows a somewhat similar behaviour to that of Muhlv, although the observed low flow pattern is rather nonlinear. There is a decrease at the beginning of the observation period followed by a flattening out after 1990. The linear trend model does not fit very well to the observed low flows which reduces the confidence one should have in this pillar. However, the observations are reproduced quite well by the stochastic projections. The slightly decrease by around 10 to 20 % until 2080. The climate scenario based rainfall runoff projections increase for the 2020–2050 period and decrease for the 2050–2080 period, the latter by about 50 to 60 %. However, the performance of the model is low as can be seen by a comparison of the simulated low flows (grey line) with the observed low flows (thin black line). As a consequence, the rainfall–runoff projections seem to be less reliable. Nevertheless, the range of different rainfall–runoff projections is still within the confidence bounds of the stochastic projections. Combining all pieces of evidences, one would expect no significant change for the 2020–2050 period (medium confidence) and a drying trend of about 20–30 % for the 2050–2080 period (low to medium confidence).

The Buwe region in the South-east gives bigger changes (Fig. 11, bottom right). The observed low flow trends are strongly influenced by the recent dry years between 2000 and 2005. This behaviour corresponds with the nonlinear, increasingly drying trend detected by Blöschl et al. (2011) and Laaha et al. (2015). However, a linear trend extrapolation of the magnitude as estimated is not very plausible given that the most recent year in the data set (2008) was less dry. The stochastic projection yields a moderately decreasing trend, which is more plausible. The change is about 15 and

HESSD
12, 13069–13122, 2015

25 % for the two projection periods. An examination of the model components suggests that the predicted changes are due to an increasing trend in temperature (Fig. 9 – right column, high confidence) and a slightly decreasing trend in precipitation (Fig. 9 – left column, medium to low confidence). The simulated signals correspond well with observed climate signals in this region. By comparison, climate projections seem to overestimate low flows for the nearer future relative to the stochastic simulations, but correspond well with the projections for 2050–2080. A regional trend analysis (Fig. 3) shows consistent behaviour in the Buwe region. Overall, there is moderate confidence in a slight drying trend for the 2020–2050 period, and a stronger drying trend of about 20–30 % for the 2050–2080 period.

8 Discussion

8.1 Realism of trend scenarios

The trend scenarios are based on the assumption that changes are linear over time. This is a simplifying view of non-stationarity which, however, is parsimonious. Although the Earth system is clearly non-linear, the annual temperatures in the European Alps have increased linearly since the mid-1970s, so a continuing trend is an obvious assumption. Similar to spatial low flow models (Laaha and Blöschl, 2006), seasonality plays an important role in the time trends of low flows. In the Alps, low flows occur in winter as a consequence of frost and snow storage and these processes are closely related to air temperature. A trend in air temperature would therefore be expected to directly translate into low flows (Blöschl and Montanari, 2010). This is borne out for the Alpine Hoalp catchment (Fig. 11, top left) which exhibits a remarkable co-behaviour with temperature.

For the other catchments that exhibit a summer low flow regime, the past changes of low flows are more subtle. Here the flow records seem too short to conclude about low flow trends, so we need additional, external information. Haslinger et al. (2014) found that the SPEI representing the net precipitation input to the catchment is a good proxy of summer low flows and this is supported by a comparison of the trends in SPEI for the summer (Fig. 2, upper panels) with the low flows in the summer dominated regions (Fig. 11, Muhlv, Gurk, Buwe). Interestingly, projected SPEI signals (Fig. 2) do not flatten out at the end as it is the case for the SPEI based on observations, and a similar effect cam be observed for low flow trends and observations. SPEI of climate scenarios are in line with low flow trends, and both point to a decrease of low flows that extends to the future. These trends are rather weak for Muhlv in the North but pronounced in Gurk in the South. For the Buwe catchment SPEI values suggest a similar decrease as Gurk basin but here the temporal pattern of low flows is different and not easy to interpret.

In all cases, the uncertainty of the trend scenarios is large, as indicated by the wide confidence bounds. It should be noted that the confidence bounds are conditional on the assumption that the linear trend model applies. If one relaxed this assumption, the bounds would be even wider. Part of the uncertainty comes from the relatively short record length (33 years). For example, Hannaford et al. (2013) have shown that low flow trends in European regimes are subject to pronounced decadal-scale variability so that even post-1960 trends (50 years) are often not consistent with the long-term picture. Laaha et al. (2015) concluded from the magnitude of decadal trend variability in Austria that more than three decades are needed for recognizing the nature of trends as a basis for obtaining robust estimates. Overall, the trend scenarios of catchments with summer low flow regime are less reliable than those for winter low flow regimes, but they do constitute a scenario of a possible future.

8.2 Uncertainty of rainfall–runoff projections

The realism of predicted impacts is also a key question for the rainfall–runoff projections based on climate scenarios. We performed an assessment of uncertainty of low flow projections, using a similar ensemble based framework as in the studies of Wong et al. (2011) for Norway, Majone et al. (2012) for the Gállego river basin in Spain, and De Wit et al. (2007) for Meuse river in France. We assessed the uncertainty arising from

HESSD
12, 13069–13122, 2015

the choice of the climate model and the emission scenario by an ensemble of three equally possible emission scenarios and two different climate models (ECHAM5 and HADCM3). Unlike De Wit et al. (2007) we did not assess possible downscaling errors as we believe that RCMs tend to play a minor role when using a delta change approach which accounts for local effects.

Uncertainty of the hydrological part of the model cascade may also be assessed by a model ensemble (e.g. Habets et al., 2013). We have chosen to focus on the parameters instead. We show, for the case study, that Q_{95} projections are sensitive not only to the selection of climate scenarios, but also to the selection of the objective function and the calibration period. The calibration uncertainty is the largest in the Alpine Hoalp basin, where the winter low flow regime is less sensitive to the projected increase of air temperature. When comparing results from different calibration periods, the effect of temporal parameter instability is clearly visible in the Buwe and Gurk basins where parameters from a colder period with less evapotranspiration tend to overestimate runoff in warmer periods. A similar effect is expected for a future, warmer climate, so the projected low flows may decrease more strongly than the projected average. This finding is in contrast with Hay et al. (2000) who identified a minor role of the hydrological model. The difference may be related to Hay et al. (2000) only assessing hydrological model performance of best-fit models and not accounting for uncertainty arising from calibration variants and time stability of model parameters. On the other hand, the finding in this paper is in line with Bosshard et al. (2013). The similarity may be due to the proximity of study areas with similar climate and catchment controls, and the similar sources of uncertainty accounted for.

Even though the analysis in this paper provides a proxy of uncertainty rather than a direct statistical measure they are considered very useful in the context of the three-pillar framework as they may assist in the process reasoning. For example, because of the more important role of air temperature in the Alpine catchments one can have higher confidence in the scenarios than in the lowlands.

HESSD
12, 13069–13122, 2015

8.3 Potential of stochastic simulations

As opposed to low flow trends and rainfall–runoff projections, which are widely used in climate impact studies of low flows, stochastic simulations are relatively rare. The main strength of the stochastic model is that it accounts for the local trends of precipitation and air temperature and captures the stochastic variability of climate. It therefore provides information complementary to that of the climate scenarios.

Extrapolating precipitation and air temperature trends involves a similar reasoning as the extrapolation of low flow trends discussed above and builds on the inertia of the climate system. Consequently, the extrapolation of temperature may be more appropriate than those of precipitation and the extrapolation into the near future may be more appropriate than those into the more distant future.

The model we use (Viglione et al., 2012) makes some simplifying assumptions which could be easily relaxed. First, the long range dependence of streamflow (Szolgayová et al., 2014) could be considered by extending the stochastic precipitation model (e.g. Thyer and Kuczera, 2003). Second, the correlations between precipitation and air temperature could be accounted for Hundecha and Merz (2012). Third, changes in seasonal temperatures could be incorporated in the model as they do seem to play a role in some of the catchments.

As the main point of the stochastic model was to illustrate the three-pillar approach, we believe that it provides an attractive method that complements the traditional climate impact studies on hydrology.

8.4 Benefits of the synthesis

The rationale of the three-pillar approach is that different data and methods of the three pillars will result in errors that are, at least partly, independent. Combining the pillars therefore involves a number of benefits.

First, the synthesis framework may assist in obtaining a judgement about the credibility of the individual approaches and increases the reliability of the overall assessment.

HESSD
12, 13069–13122, 2015

For the case study catchment Muhlv in the region north of the Alps, consistently small changes are predicted by all methods. The fact that all methods yield similar results adds credence to all projections as they support each other.

Second, the synthesis may contribute to a better understanding of the response of low flow regimes to a future changed climate. For the case study catchment Buwe in the Southeast, for example, the observed low flow signal shows a non-linear drying trend. An examination of the model components of the stochastic projections suggests that the predicted changes are due to an increasing trend in temperature and a slightly decreasing trend in precipitation. GCM scenarios correspond well with these trends, and this in turn lends a relatively high credence to the rainfall–runoff projections of climate scenarios.

Third, it is believed that the three pillar approach allows for a more complete way of assessing the uncertainty of the projections. For the case study catchment Hoalp in the Alpine region, trend projections and climate scenarios yield consistent projections of increasing low flows, although of different magnitudes. The inter-comparison of all projection methods including process reasoning in every analysis step enables us to better assess their individual uncertainties. This information is vital for weighting the projections when performing a synthesis, to gain a more informed estimate of expected changes and their uncertainties. For predicting near-future low flows in the Hoalp catchment, the trend model appears most reliable and receives most weight. From trend predictions alone one would conclude an increase by +42 % but with a very wide range of uncertainty (about ±100 % of the expected value), so one would have low confidence in the absolute figures of projected change. Additional information from rainfall runoff projections (that suggest an increase of about 15 to 30 %) has been useful to constrain the projected increase to about 20 to 40 %. The more complete information reduces the uncertainty of projected changes and this increases our confidence in low flow projections.

In the context of water resources management, all three benefits are considered to be relevant. Decision makers are usually reluctant to use the output from black

HESSD
12, 13069–13122, 2015

box models as the sole basis of their decisions. Just as important as the expected changes in the water system are the uncertainties associated with the changes as well as a process reasoning in terms of cause and effect. This is particular the case if robust drought management strategies, such as the vulnerability approach, are to be adopted. The vulnerability approach differs from the predictive climate scenario approach in that it aims at reducing vulnerability and enhancing resilience of the water system (Wilby and Dessai, 2010; Blöschl et al., 2013). Typically, the strategies are not optimal from an economical perspective but they are robust, i.e. they are designed to perform well over a wide range of assumptions about the future and potentially extremely negative effects. Central to the approach is an understanding of the cause–effect relationships within the water system under a variety of conditions, as well as an appreciation of the possible uncertainties. For example, Watts et al. (2012) tested the resilience of drought plans in England to droughts that are outside recent experience using nineteenth century drought records. Methods often involve exploratory modelling approaches which fit well with the three pillar approach proposed here. We therefore believe that the approach put forward in this paper can play an important role in assisting risk managers in developing drought management strategies for the practice.

9 Conclusions

In this paper, we propose a framework that combines low flow projections from different sources of information. These pillars of information are trends in observed low flows, rainfall–runoff projections based on climate scenarios, and stochastic projections based on local hydro-meteorological data. The pillars are either observation-based or process-based and therefore combine elements of upward and downward approaches in hydrology.

The methodology is demonstrated for four example catchments in Austria that represent typical climate conditions in Central Europe. The results of the individual projections sometimes differ in terms of their signs and magnitudes, mainly depending on

HESSD
12, 13069–13122, 2015

the dominant low flow seasonality. For the Alpine region where winter low flows dominate, trend projections and climate scenarios yield consistent projections of a wetting trend but of different magnitudes. For the region north of the Alps, all methods project rather small changes. For the regions in the South and Southeast more pronounced and mostly decreasing trends are projected but there is disagreement in the magnitude of the projected changes.

The systematic combination of different sources of information in the framework of the three-pillar approach offers a number of opportunities for drought projections: (i) checking the plausibility of individual projections and improving the reliability of the overall assessment, (ii) understanding the cause–effect relationships involved, and (iii) enhancing the understanding of the uncertainties of the assessment based on the consistency of the individual pillars.

Application to the case study catchments suggest that the approach is viable. As the methods and information used in each pillar are largely independent from each other, the combined assessment is likely more accurate than each of the individual projections. The synthesis or combination of information may be performed by expert judgement as shown in this paper. Alternatively, more formal methods exist which could also be used. In all cases, the confidence in the combined projection will depend on how closely the pillars agree, and on the individual uncertainties.

Future work may be directed towards adding historic information as an additional pillar. Historic information may come from archival data, tree ring analysis and other sources. They would allow assessment of a still wider spectrum of conditions than those analysed in this paper and may contribute additional benefits to water management decisions.

HESSD
12, 13069–13122, 2015

Acknowledgements. The paper is a contribution to UNESCO's FRIEND-Water program. The authors would like to thank the Austrian Climate Research Program ACRP for financial support through the projects CILFAD (GZ B060 362) and DALF-Pro (GZ B464 822), and the Austrian Academy of Sciences for financial support through the "Predictability of Runoff" project. We thank the Central Institute for Meteorology and Geodynamics (ZAMG) and the Hydrographical Service of Austria (HZB) for providing meteorological and hydrological data, and Tobias Gauster for help with Fig. 11.

References

Auer, I., Böhm, R., Jurkovic, A., Lipa, W., Orlik, A., Potzmann, R., Schöner, W., Ungersböck, M., Matulla, C., Briffa, K., Jones, P., Efthymiadis, D., Brunetti, M., Nanni, T., Maugeri, M., Mercalli, L., Mestre, O., Moisselin, J.-M., Begert, M., Müller-Westermeier, G., Kveton, V., Bochnicek, O., Stastny, P., Lapin, M., Szalai, S., Szentimrey, T., Cegnar, T., Dolinar, M., Gajic-Capka, M., Zaninovic, K., Majstorovic, Z., and Nieplova, E.: HISTALP – historical instrumental climatological surface time series of the Greater Alpine Region, Int. J. Climatol., 27, 17–46, doi:10.1002/joc.1377, 2007.

Blöschl, G. and Montanari, A.: Climate change impacts – throwing the dice?, Hydrol. Process., 24, 374–381, 2010.

Blöschl, G., Viglione, A., Merz, R., Parajka, J., Salinas, J. L., and Schöner, W.: Auswirkungen des Klimawandels auf Hochwasser und Niederwasser, Österr. Wasser-Abfallwirt., 63, 21–30, 2011.

Blöschl, G., Viglione, A., and Montanari, A.: Emerging approaches to hydrological risk management in a changing world, in: Climate Vulnerability, Elsevier, 3–10, available at: http://linkinghub.elsevier.com/retrieve/pii/B9780123847034005050 (last access: 3 November 2015), 2013.

Böhm, R., Auer, I., Brunetti, M., Maugeri, M., Nanni, T., and Schöner, W.: Regional temperature variability in the European Alps: 1760–1998 from homogenized instrumental time series, Int. J. Climatol., 21, 1779–1801, doi:10.1002/joc.689, 2001.

Bosshard, T., Carambia, M., Goergen, K., Kotlarski, S., Krahe, P., Zappa, M., and Schär, C.: Quantifying uncertainty sources in an ensemble of hydrological climate-impact projections, Water Resour. Res., 49, 1523–1536, doi:10.1029/2011WR011533, 2013.

Ceola, S., Arheimer, B., Baratti, E., Blöschl, G., Capell, R., Castellarin, A., Freer, J., Han, D., Hrachowitz, M., Hundecha, Y., Hutton, C., Lindström, G., Montanari, A., Nijzink, R., Parajka, J., Toth, E., Viglione, A., and Wagener, T.: Virtual laboratories: new opportunities for collaborative water science, Hydrol. Earth Syst. Sci., 19, 2101–2117, doi:10.5194/hess-19-2101-2015, 2015.

Chauveau, M., Chazot, S., Perrin, C., Bourgin, P.-Y., Sauquet, E., Vidal, J.-P., Rouchy, N., Martin, E., David, J., Norotte, T., Maugis, P., and De Lacaze, X.: Quels impacts des changements climatiques sur les eaux de surface en France à l'horizon 2070?, Houille Blanche, 4, 5–15, doi:10.1051/lhb/2013027, 2013.

De Wit, M. J. M., Van den Hurk, B., Warmerdam, P. M. M., Torfs, P. J. J. F., Roulin, E., and Van Deursen, W. P. A.: Impact of climate change on low-flows in the river Meuse, Climatic Change, 82, 351–372, doi:10.1007/s10584-006-9195-2, 2007.

Diaz-Nieto, J. and Wilby, R. L.: A comparison of statistical downscaling and climate change factor methods: impacts on low flows in the River Thames, UK, Climatic Change, 69, 245–268, 2005.

Douglas, E., Vogel, R., and Kroll, C.: Trends in floods and low flows in the United States: impact of spatial correlation, J. Hydrol., 240, 90–105, 2000.

Duan, Q., Sorooshian, S., and Gupta, V.: Effective and efficient global optimization for conceptual rainfall–runoff models, Water Resour. Res., 28, 1015–1031, 1992.

Field, C. B. and Intergovernmental Panel on Climate Change: Managing the Risks of Extreme Events and Disasters to Advance Climate Change Adaption: Special Report of the Intergovernmental Panel on Climate Change, Cambridge University Press, New York, 2012.

Gaál, L., Szolgay, J., Kohnová, S., Parajka, J., Merz, R., Viglione, A., and Blöschl, G.: Flood timescales: understanding the interplay of climate and catchment processes through comparative hydrology, Water Resour. Res., 48, W04511, doi:10.1029/2011WR011509, 2012.

Giuntoli, I., Renard, B., Vidal, J.-P., and Bard, A.: Low flows in France and their relationship to large-scale climate indices, J. Hydrol., 482, 105–118, doi:10.1016/j.jhydrol.2012.12.038, 2013.

Gupta, H. V., Blöschl, G., McDonnel, J., Savenije, H., Sivapalan, M., Viglione, A., and Wagener, T.: Synthesis, in: chapter 12, Runoff Prediction in Ungauged Basins – Synthesis across Processes, Places and Scales, edited by: Blöschl, G., Sivapalan, M., Wagener, T., Viglione, A., and Savenije, H., Cambridge University Press, Cambridge, UK, 361–383, 2013.

HESSD
12, 13069–13122, 2015

Gutknecht, D., Blöschl, G., Reszler, C., and Heindl, H.: Ein "Mehr-Standbeine"-Ansatz zur Ermittlung von Bemessungshochwässern kleiner Auftretenswahrscheinlichkeit, Österr. Wasser-Abfallwirt., 58, 44–50, 2006.

Habets, F., Boé, J., Déqué, M., Ducharne, A., Gascoin, S., Hachour, A., Martin, E., Pagé, C., Sauquet, E., Terray, L., Thiéry, D., Oudin, L., and Viennot, P.: Impact of climate change on the hydrogeology of two basins in northern France, Climatic Change, 121, 771–785, doi:10.1007/s10584-013-0934-x, 2013.

Hall, J., Arheimer, B., Borga, M., Brázdil, R., Claps, P., Kiss, A., Kjeldsen, T. R., Kriaučiūnienė, J., Kundzewicz, Z. W., Lang, M., Llasat, M. C., Macdonald, N., McIntyre, N., Mediero, L., Merz, B., Merz, R., Molnar, P., Montanari, A., Neuhold, C., Parajka, J., Perdigão, R. A. P., Plavcová, L., Rogger, M., Salinas, J. L., Sauquet, E., Schär, C., Szolgay, J., Viglione, A., and Blöschl, G.: Understanding flood regime changes in Europe: a state-of-the-art assessment, Hydrol. Earth Syst. Sci., 18, 2735–2772, doi:10.5194/hess-18-2735-2014, 2014.

Hannaford, J. and Buys, G.: Trends in seasonal river flow regimes in the UK, J. Hydrol., 475, 158–174, 2012.

Hannaford, J., Buys, G., Stahl, K., and Tallaksen, L. M.: The influence of decadal-scale variability on trends in long European streamflow records, Hydrol. Earth Syst. Sci., 17, 2717–2733, doi:10.5194/hess-17-2717-2013, 2013.

Haslinger, K., Anders, I., and Hofstätter, M.: Regional climate modelling over complex terrain: an evaluation study of COSMO-CLM hindcast model runs for the Greater Alpine Region, Clim. Dynam., 40, 511–529, 2013.

Haslinger, K., Koffler, D., Schöner, W., and Laaha, G.: Exploring the link between meteorological drought and streamflow: effects of climate-catchment interaction, Water Resour. Res., 50, 2468–2487, doi:10.1002/2013WR015051, 2014.

Hay, L. E., Wilby, R. L., and Leavesley, G. H.: A comparison of delta change and downscaled GCM scenarios for three mountainous basins in the United States, J. Am. Water Resour. As., 36, 387–397, 2000.

Hundecha, Y. and Merz, B.: Exploring the relationship between changes in climate and floods using a model-based analysis, Water Resour. Res., 48, W04512, doi:10.1029/2011WR010527, 2012.

HESSD
12, 13069–13122, 2015

Hurkmans, R., Terink, W., Uijlenhoet, R., Torfs, P., Jacob, D., and Troch, P. A.: Changes in streamflow dynamics in the Rhine basin under three high-resolution regional climate scenarios, J. Climate, 23, 679–699, 2010.
Kuczera, G.: Combining site-specific and regional information: an empirical Bayes Approach, Water Resour. Res., 18, 306–314, 1982.
Laaha, G. and Blöschl, G.: Seasonality indices for regionalizing low flows, Hydrol. Process., 20, 3851–3878, doi:10.1002/hyp.6161, 2006.
Laaha, G. and Blöschl, G.: A national low flow estimation procedure for Austria, Hydrolog. Sci. J., 52, 625–644, 2007.
Laaha, G., Koffler, D., Zehetgruber, Judith, Haslinger, K., Schöner, W., Parajka, J., Viglione, A., and Blöschl, G.: Low flow trends in Austria from local and regional information, Hydrol. Earth Syst. Sci., in preparation, 2015.
Lins, H. F. and Slack, J. R.: Streamflow trends in the United States, Geophys. Res. Lett., 26, 227–230, 1999.
Loibl, W., Formayer, H., Schöner, W., Truhetz, H., Anders, I., Gobiet, A., Heinrich, G., Köstl, M., Nadeem, I., Peters-Anders, J., Schicker, I., Suklitsch, M. and Züger, H.: Reclip: century 1 Research for climate protection – century climate simulations: Models, Data and GHG-Scenarios, Simulations, Project Report, AIT – Austrian Institute of Technology, Vienna, 2011.
Lorenzo-Lacruz, J., Vicente-Serrano, S. M., López-Moreno, J. I., Morán-Tejeda, E., and Zabalza, J.: Recent trends in Iberian streamflows (1945–2005), J. Hydrol., 414, 463–475, doi:10.1016/j.jhydrol.2011.11.023, 2012.
Majone, B., Bovolo, C. I., Bellin, A., Blenkinsop, S., and Fowler, H. J.: Modeling the impacts of future climate change on water resources for the Gállego river basin (Spain), Water Resour. Res., 48, W01512, doi:10.1029/2011WR010985, 2012.
Merz, R. and Blöschl, G.: Flood frequency hydrology: 2. Combining data evidence, Water Resour. Res., 44, W08433, doi:10.1029/2007WR006745, 2008.
Merz, R., Parajka, J., and Blöschl, G.: Time stability of catchment model parameters: implications for climate impact analyses, Water Resour. Res., 47, W02531, doi:10.1029/2010WR009505, 2011.
Parajka, J., Merz, R., and Blöschl, G.: Uncertainty and multiple objective calibration in regional water balance modelling: case study in 320 Austrian catchments, Hydrol. Process., 21, 435–446, doi:10.1002/hyp.6253, 2007.

HESSD
12, 13069–13122, 2015

A three-pillar approach to assessing climate impacts on low flows

G. Laaha et al.

Parajka, J., Blaschke, A. P., Blöschl, G., Haslinger, K., Hepp, G., Laaha, G., Schöner, W., Trautvetter, H., Viglione, A., and Zessner, M.: Uncertainty contributions to low flow projections in Austria, Hydrol. Earth Syst. Sci. Discuss., 12, 12395–12431, doi:10.5194/hessd-12-12395-2015, 2015.
Prudhomme, C., Young, A., Watts, G., Haxton, T., Crooks, S., Williamson, J., Davies, H., Dadson, S., and Allen, S.: The drying up of Britain? A national estimate of changes in seasonal river flows from 11 Regional Climate Model simulations, Hydrol. Process., 26, 1115–1118, doi:10.1002/hyp.8434, 2012.
Prudhomme, C., Giuntoli, I., Robinson, E. L., Clark, D. B., Arnell, N. W., Dankers, R., Fekete, B. M., Franssen, W., Gerten, D., Gosling, S. N., Hagemann, S., Hannah, D. M., Kim, H., Masaki, Y., Satoh, Y., Stacke, T., Wada, Y., and Wisser, D.: Hydrological droughts in the 21st century, hotspots and uncertainties from a global multimodel ensemble experiment, P. Natl. Acad. Sci. USA, 111, 3262–3267, doi:10.1073/pnas.1222473110, 2014.
Renard, B., Lang, M., Bois, P., Dupeyrat, A., Mestre, O., Niel, H., Sauquet, E., Prudhomme, C., Parey, S., Paquet, E., Neppel, L., and Gailhard, J.: Regional methods for trend detection: assessing field significance and regional consistency, Water Resour. Res., 44, W08419, doi:10.1029/2007WR006268, 2008.
Schöner, W., Böhm, R., and Auer, I.: 125 years of high-mountain research at Sonnblick Observatory (Austrian Alps) – from "the house above the clouds" to a unique research platform, Theor. Appl. Climatol., 110, 491–498, 2012.
Sheffield, J., Wood, E. F., and Roderick, M. L.: Little change in global drought over the past 60 years, Nature, 491, 435–438, 2012.
Sivapalan, M., Blöschl, G., Zhang, L., and Vertessy, R.: Downward approach to hydrological prediction, Hydrol. Process., 17, 2101–2111, doi:10.1002/hyp.1425, 2003.
Sivapalan, M., Blöschl, G., Merz, R., and Gutknecht, D.: Linking flood frequency to long-term water balance: incorporating effects of seasonality, Water Resour. Res., 41, W06012, doi:10.1029/2004WR003439, 2005.
Stahl, K., Hisdal, H., Hannaford, J., Tallaksen, L. M., van Lanen, H. A. J., Sauquet, E., Demuth, S., Fendekova, M., and Jódar, J.: Streamflow trends in Europe: evidence from a dataset of near-natural catchments, Hydrol. Earth Syst. Sci., 14, 2367–2382, doi:10.5194/hess-14-2367-2010, 2010.
Stedinger, J. R. and Tasker, G. D.: Regional hydrologic analysis: 1. Ordinary, weighted, and generalized least squares compared, Water Resour. Res., 21, 1421–1432, 1985.

HESSD
12, 13069–13122, 2015

Szolgayová, E., Laaha, G., Blöschl, G., and Bucher, C.: Factors influencing long range dependence in streamflow of European rivers, Hydrol. Process., 28, 1573–1586, 2014.
Thyer, M. and Kuczera, G.: A hidden Markov model for modelling long-term persistence in multi-site rainfall time series, 1. Model calibration using a Bayesian approach, J. Hydrol., 275, 12–26, 2003.
Van Loon, A. F. and Laaha, G.: Hydrological drought severity explained by climate and catchment characteristics, J. Hydrol., 526, 3–14, doi:10.1016/j.jhydrol.2014.10.059, 2015.
Vicente-Serrano, S. M., Beguería, S., and López-Moreno, J. I.: A multiscalar drought index sensitive to global warming: the standardized precipitation evapotranspiration index, J. Climate, 23, 1696–1718, 2010.
Viglione, A. and Parajka, J.: TUWmodel: Lumped Hydrological Model for Education Purposes, R package, available at: http://CRAN.R-project.org/package=TUWmodel (last access: 15 October 2015), 2014.
Viglione, A., Castellarin, A., Rogger, M., Merz, R., and Blöschl, G.: Extreme rainstorms: comparing regional envelope curves to stochastically generated events, Water Resour. Res., 48, W01509, doi:10.1029/2011WR010515, 2012.
Viglione, A., Merz, R., Salinas, J. L., and Blöschl, G.: Flood frequency hydrology: 3. a Bayesian analysis, Water Resour. Res., 49, 675–692, doi:10.1029/2011WR010782, 2013.
Watts, G., von Christierson, B., Hannaford, J., and Lonsdale, K.: Testing the resilience of water supply systems to long droughts, J. Hydrol., 414, 255–267, 2012.
Wilby, R. L. and Dessai, S.: Robust adaptation to climate change, Weather, 65, 180–185, 2010.
Wilson, D., Hisdal, H., and Lawrence, D.: Has streamflow changed in the Nordic countries? – Recent trends and comparisons to hydrological projections, J. Hydrol., 394, 334–346, doi:10.1016/j.jhydrol.2010.09.010, 2010.
Winsemius, H. C., Schaefli, B., Montanari, A., and Savenije, H. H. G.: On the calibration of hydrological models in ungauged basins: a framework for integrating hard and soft hydrological information, Water Resour. Res., 45, W12422, doi:10.1029/2009WR007706, 2009.
Wong, W. K., Beldring, S., Engen-Skaugen, T., Haddeland, I., and Hisdal, H.: Climate change effects on spatiotemporal patterns of hydroclimatological summer droughts in Norway, J. Hydrometeorol., 12, 1205–1220, doi:10.1175/2011JHM1357.1, 2011.
Yue, S., Pilon, P., Phinney, B., and Cavadias, G.: The influence of autocorrelation on the ability to detect trend in hydrological series, Hydrol. Process., 16, 1807–1829, 2002.

HESSD
12, 13069–13122, 2015

HESSD
12, 13069–13122, 2015

Table 1. Trend estimates of observed low flows in the period 1976–2008 (Mann–Kendall test). Relative trends refer to the trend over the observation period relative to its mean.

	Hoalp	Muhlv	Gurk	Buwe
Trend ($m^3 s^{-1}$ per 100 years)	+0.24	−0.28	−1.45	−0.34
Relative trend (% per year)	+1.21	−0.38	−0.78	−1.88
p value	0.009	0.377	0.053	0.045
p value prewhitened	0.003	0.250	0.178	0.058
Significance	**			*

Significance codes: ** < 0.05; * < 0.01.

Table 2. Trend predictions of average Q_{95} low flows ($m^3 s^{-1}$) for the periods 2021–2050 and 2051–2080 based on extending observed trends. Predicted changes (%) relative to average low flow discharge Q_{95} of the reference period (1976–2008). Values in parenthesis refer to the 95 % confidence interval.

	Hoalp	Muhlv	Gurk	Buwe
2021–2050				
Q_{95}	0.28 (0.19, 0.38)	0.67 (0.36, 0.97)	1.17 (0.48, 1.87)	0.02 (−0.10, 0.14)
Change	+42 (−5, +88)	−10 (−51, +32)	−36 (−74, +1)	−89 (−156, −21)
2051–2080				
Q_{95}	0.35 (0.20, 0.51)	0.58 (0.07, 1.09)	0.74 (−0.42, 1.90)	−0.08 (−0.29, 0.12)
Change	+78 (+1, +156)	−21 (−91, +48)	−60 (−123, +3)	−145 (−258, −33)

HESSD
12, 13069–13122, 2015

Table 3. Runoff model efficiency Z_Q (Eq. 4) obtained for different weights w_Q (Eq. 4) in four selected basins for three different calibration periods. Z_Q are listed in the sequence of the calibration periods: 1976–1986/1987–1997/1998–2008.

w_Q	Hoalp	Muhlv	Gurk	Buwe
0.0	0.96/0.95/0.90	0.82/0.84/0.86	0.79/0.73/0.79	0.46/0.52/0.59
0.1	0.95/0.93/0.90	0.81/0.83/0.86	0.79/0.73/0.79	0.37/0.52/0.58
0.2	0.94/0.92/0.90	0.80/0.82/0.86	0.78/0.74/0.79	0.35/0.53/0.58
0.3	0.93/0.90/0.90	0.79/0.81/0.86	0.78/0.74/0.79	0.34/0.54/0.58
0.4	0.92/0.89/0.89	0.79/0.80/0.86	0.78/0.74/0.79	0.40/0.54/0.57
0.5	0.91/0.88/0.89	0.77/0.79/0.86	0.78/0.75/0.78	0.36/0.55/0.56
0.6	0.90/0.86/0.89	0.77/0.78/0.86	0.78/0.75/0.78	0.30/0.56/0.55
0.7	0.89/0.85/0.89	0.76/0.78/0.86	0.78/0.75/0.78	0.30/0.57/0.55
0.8	0.88/0.83/0.75	0.76/0.77/0.81	0.78/0.76/0.80	0.30/0.58/0.49
0.9	0.88/0.82/0.73	0.75/0.76/0.81	0.78/0.76/0.80	0.28/0.59/0.49
1.0	0.87/0.82/0.72	0.75/0.75/0.81	0.78/0.77/0.81	0.29/0.60/0.49

HESSD
12, 13069–13122, 2015

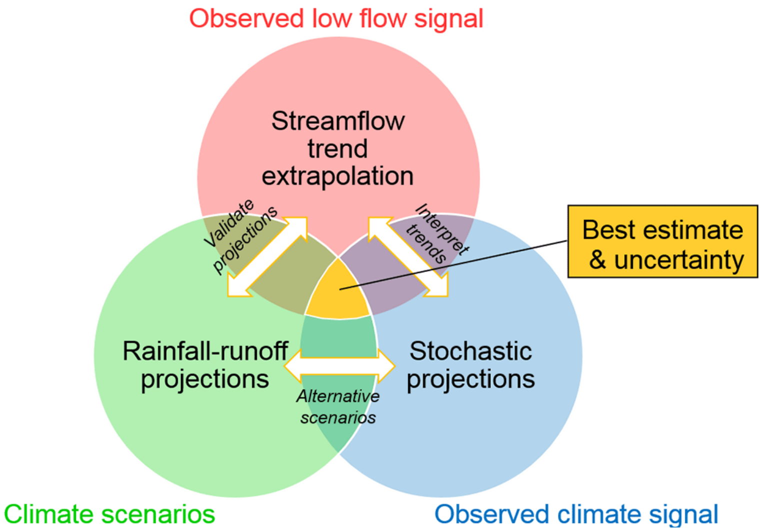

Figure 1. Three-pillar approach of low flow projection: the first pillar, streamflow trend extrapolation, exploits information of the observed low flow signal. The second pillar, rainfall–runoff projections, exploits information of climate scenarios. The third pillar, stochastic projections, extrapolates trends of observed climate signals. Intercomparisons (indicated by arrows) allow interpretation of trends, validation of rainfall–runoff projections, and alternative scenarios. The combination of the three pieces of information yields estimates consistent with all the information, together with an appreciation of their uncertainty.

HESSD
12, 13069–13122, 2015

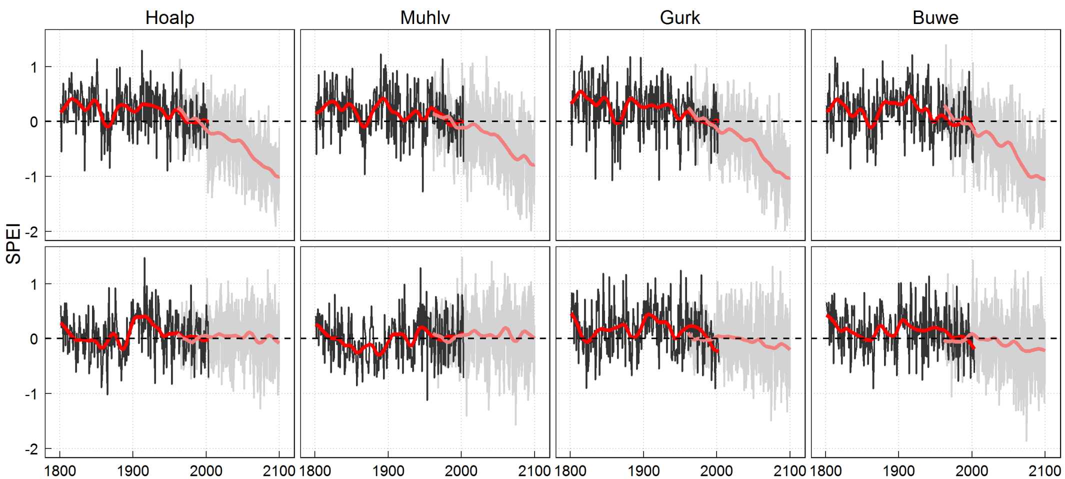

Figure 2. Observed (HISTALP, black) and projected (reclip: century ensemble spread, grey) evolution of the standardized precipitation evaporation index SPEI in summer (upper panels) and winter (lower panels) for the four example catchments in Austria; the red and light red lines represent the Gaussian low-pass filter of the observed and projected SPEI time series, respectively.

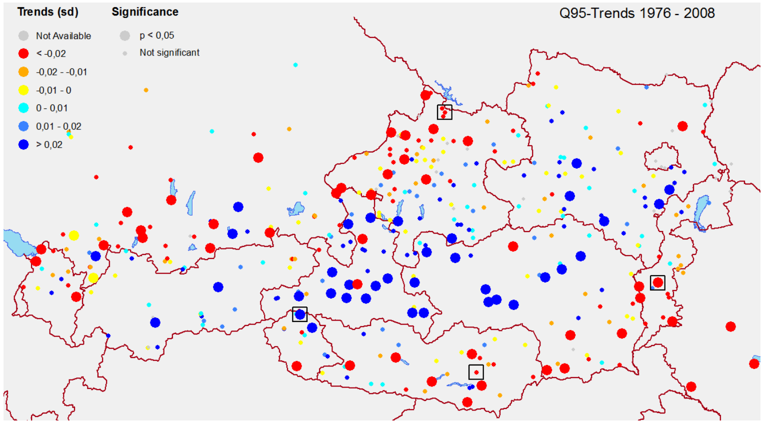

Figure 3. Observed trends of Q_{95} low flows in Austria in the period 1976–2008. Colours correspond to the sign and the magnitude of the trends (blue = increasing, red = decreasing). Size indicates significance of trends. Units of the trends are standard deviations per year. Squares indicate example catchments; West: Tauernbach at Matreier Tauernhaus (Hoalp); North: Steinerne Mühl at Harmannsdorf (Muhlv): South: Glan at Zollfeld (Gurk); East: Tauchenbach at Altschlaining (Buwe) (from Laaha et al., 2015).

HESSD
12, 13069–13122, 2015

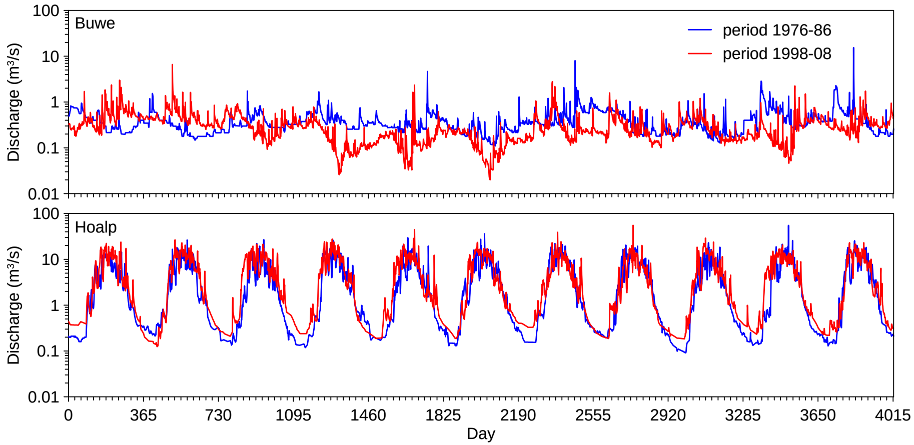

Figure 4. Observed daily discharge for the periods 1976–1986 (blue line) and 1998–2008 (red line) in the Buwe (upper panel) and Hoalp (bottom panel) basins.

HESSD
12, 13069–13122, 2015

A three-pillar approach to assessing climate impacts on low flows

G. Laaha et al.

Title Page
Abstract | Introduction
Conclusions | References
Tables | Figures
◀| |▶
◀ ▶
Back | Close
Full Screen / Esc
Printer-friendly Version
Interactive Discussion

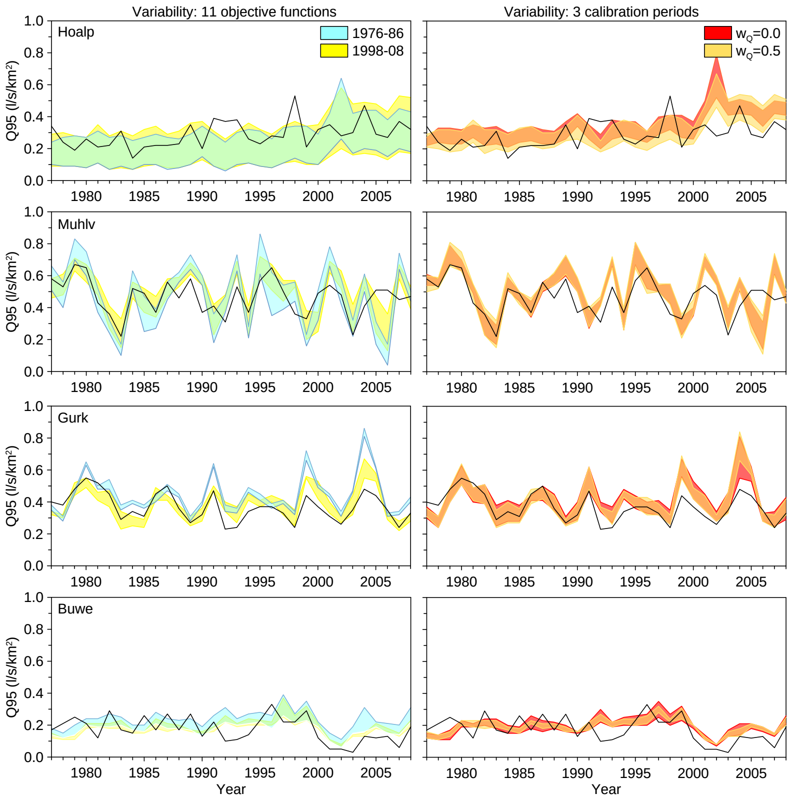

Figure 5. Annual low flow quantiles Q_{95} estimated from observed data (black line) and from hydrologic model simulations (coloured bands). Band widths in the left panels show variability due to different weights in the objective function for two calibration periods (1976–1986 and 1998–2008). Band widths in the right panels show variability due to different decades used for model calibration for two sets of weights ($w_Q = 0.5$ and $w_Q = 0.0$).

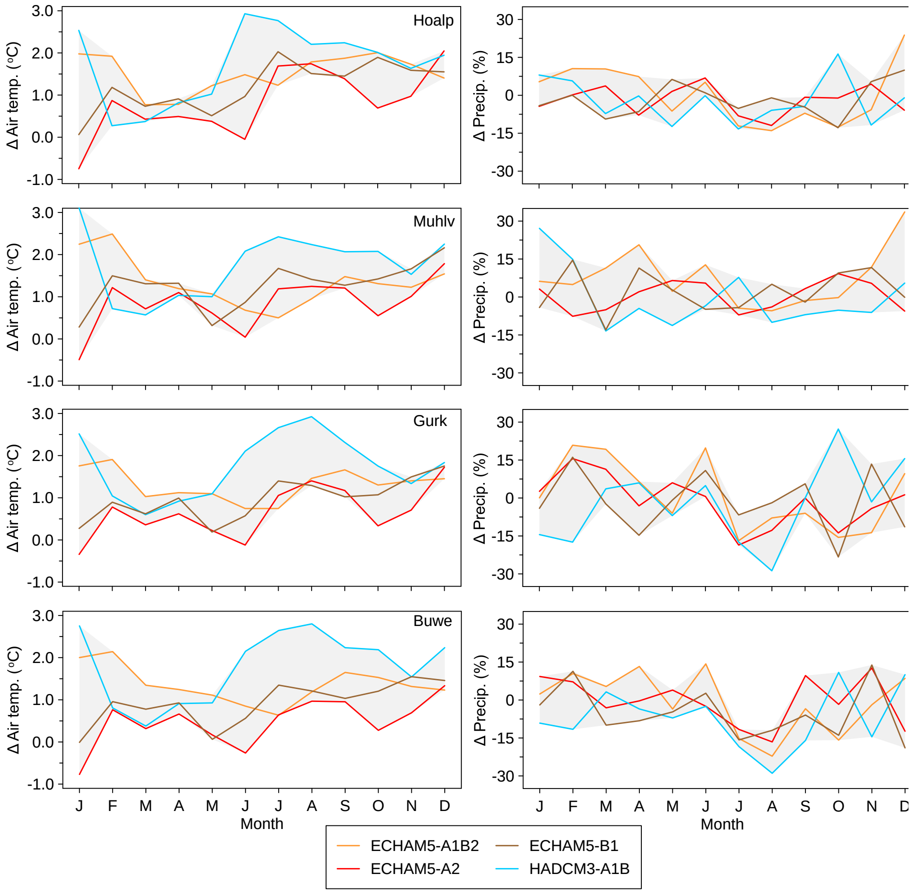

Figure 6. Projections of air temperatures and precipitation for four basins in Austria simulated by regional climate models. Shown are long-term monthly changes of the future period (2021–2050) relative to the reference period (1976–2008). Shaded area indicates the range of climate scenarios/models.

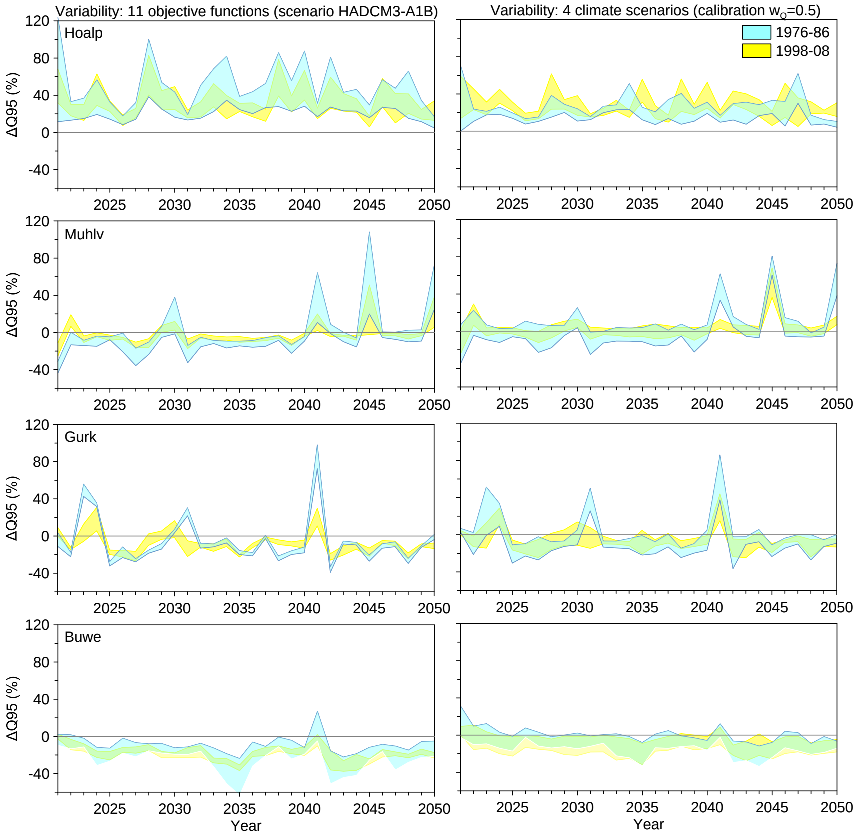

Figure 7. Projections of Q_{95} low flows for four basins in Austria in terms of the changes of the future period (2021–2050) relative to the reference period (1976–2008). Band widths in the left panels show the variability due to 11 calibration variants for HADCM3. Band widths in the right panels show the variability due to the choice of climate projections for calibration variant $w_Q = 0.5$. Yellow and blue colours relate to two calibration periods for the hydrological model.

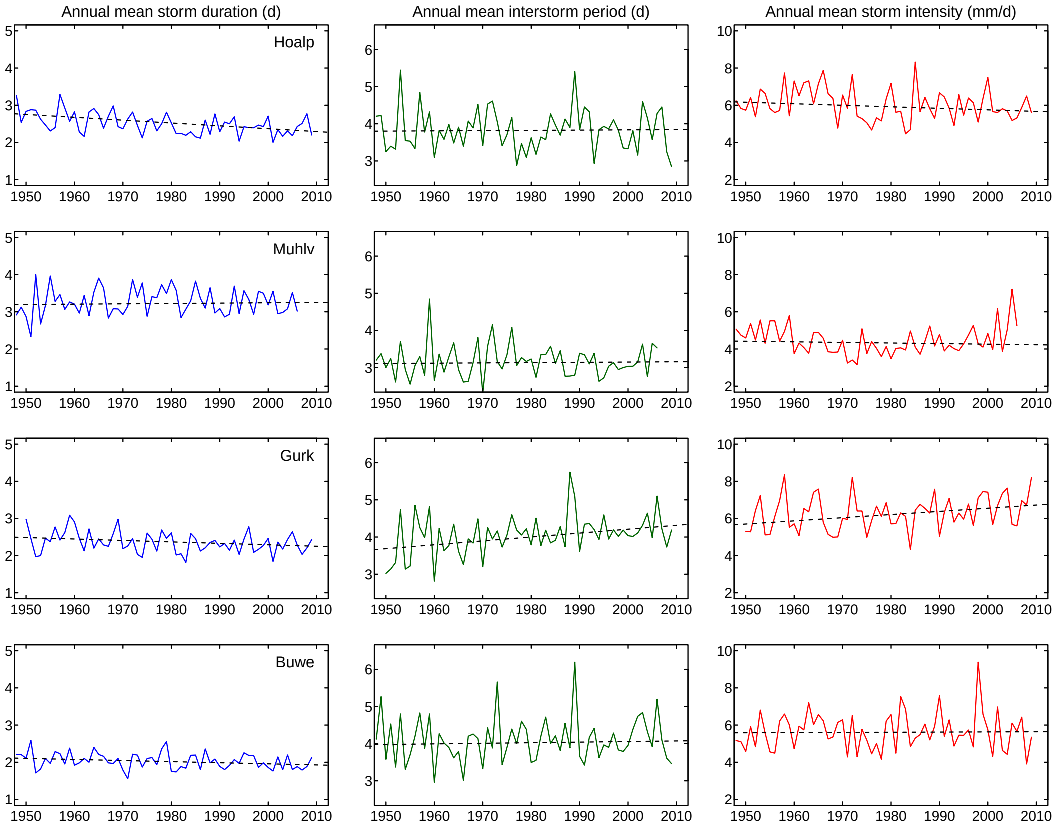

Figure 8. Observed trend in the precipitation statistics for the climate stations: St. Jakob Def (Hoalp), Pabneukirchen (Muhlv), Klagenfurt (Gurk), Woerterberg (Buwe). The trend lines have been fitted with the Theil–Sen method.

HESSD
12, 13069–13122, 2015

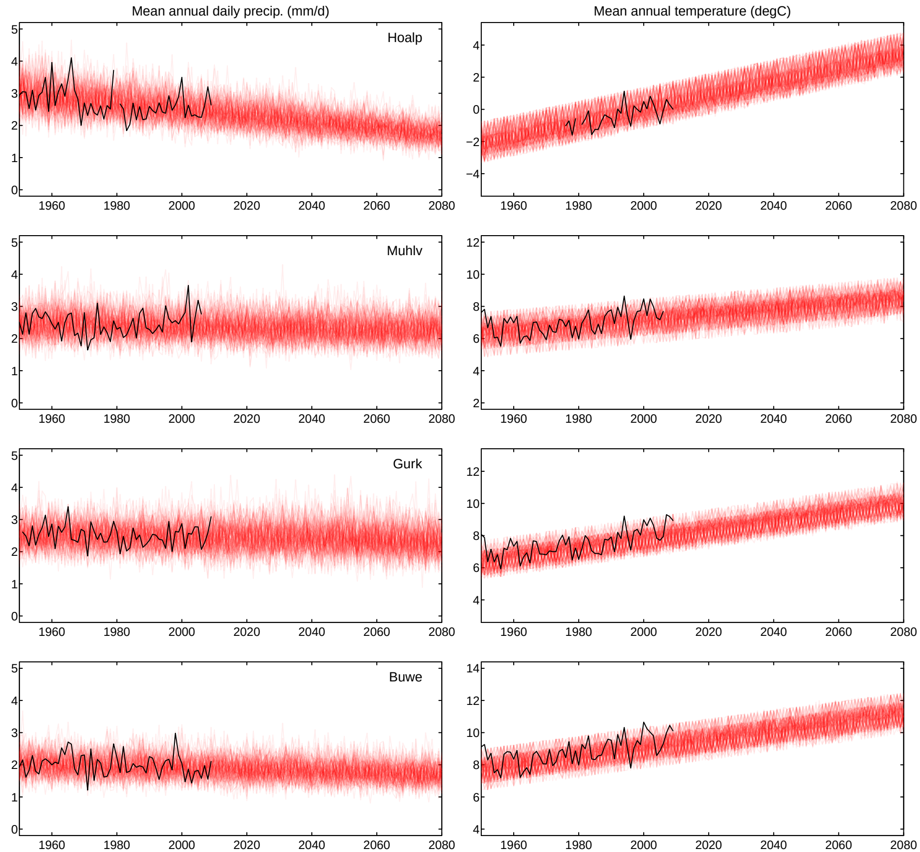

Figure 9. Stochastic simulations of mean annual daily precipitation and mean annual temperature (red lines) for St. Jakob Def (Hoalp), Pabneukirchen (Muhlv), Klagenfurt (Gurk), Woerterberg (Buwe). 100 simulated time series for each station. For comparison observations are shown (black lines).

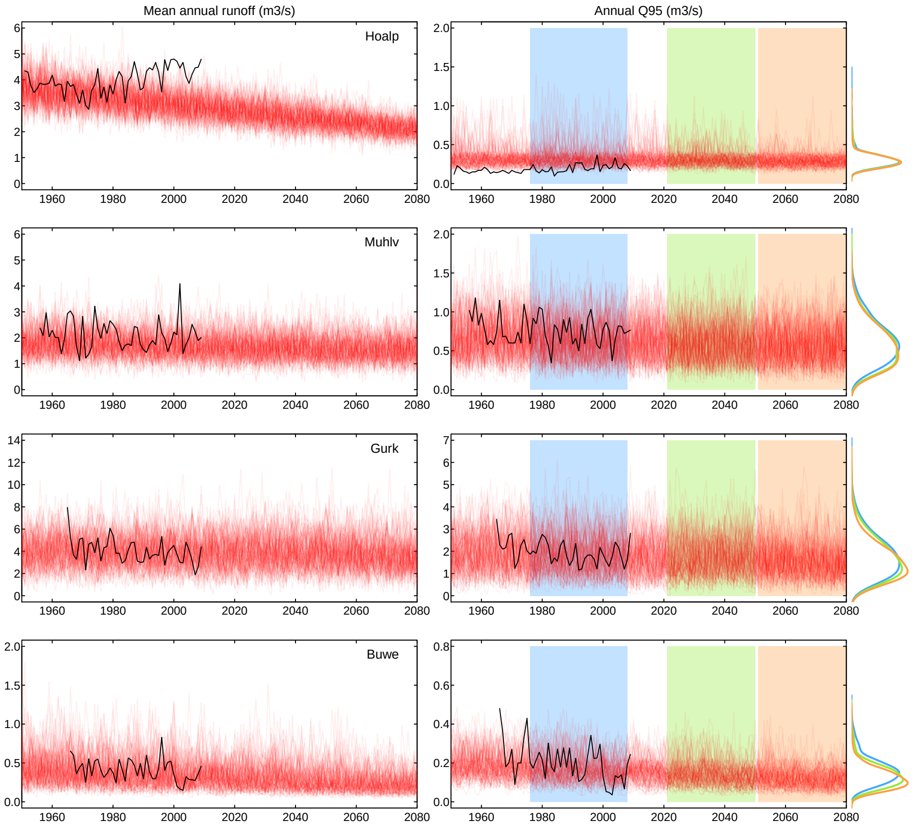

Figure 10. Stochastic simulations of mean annual runoff and annual Q_{95} (red lines) assuming linear extrapolation of the rainfall model parameters for Tauernbach at Matreier Tauernhaus (Hoalp), Steinerne Mühl at Harmannsdorf (Muhlv), Glan at Zollfeld (Gurk), and Tauchenbach at Altschlaining (Buwe). 100 simulated time series for each catchment. For comparison observations are shown (black lines). Density distributions of Q_{95} for three periods are shown on the right.

HESSD
12, 13069–13122, 2015

A three-pillar approach to assessing climate impacts on low flows

G. Laaha et al.

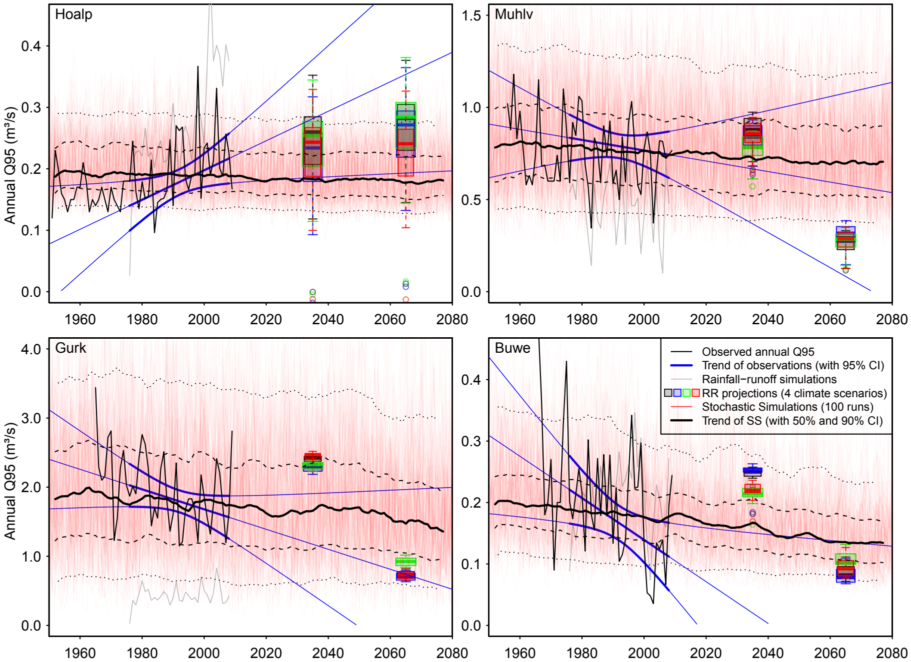

Figure 11. Three-pillar projections of low flows Q_{95} for the four example catchments: Tauernbach at Matreier Tauernhaus (Hoalp), Steinerne Mühl at Harmannsdorf (Muhlv), Glan at Zollfeld (Gurk), and Tauchenbach at Altschlaining (Buwe). Black lines refer to observed annual Q_{95}. Pillar 1: trend line (blue) and 0.95 level confidence bounds (blue curved lines); bold/thin parts refer to observation/extrapolation period. Pillar 2: simulated Q_{95} for observation period (gray line) and climate scenario based average Q_{95} for 2021–2050 and 2051–2080 (box plots, colours indicate different climate scenarios, range of box plots indicates different parameters of the hydrological model) Pillar 3: stochastic simulations of Q_{95} (100 realisations, red lines) assuming linear extrapolation of rainfall model parameters with 0.50 level confidence bounds (black dashed lines) and 0.90 level confidence bounds (black dotted lines).